Supplement of Earth Syst. Dynam., 6, 447–460, 2015
http://www.earth-syst-dynam.net/6/447/2015/
doi:10.5194/esd-6-447-2015-supplement

Earth System Dynamics
Open Access

Supplement of

A framework for the cross-sectoral integration of multi-model impact projections: land use decisions under climate impacts uncertainties

K. Frieler et al.

Correspondence to: K. Frieler (katja.frieler@pik-potsdam.de)

Supplement of

A framework for the cross-sectoral integration of multi-model impact projections: Land use decisions under climate impacts uncertainties

1 Short descriptions of the Global Gridded Crop Models (GGCM)

model	CO_2 fertilization	Fertilizer use	Adaptation	starting conditions (representation of present day yields or potential yields?)
EPIC (Izaurralde et al., 2006; Williams, 1995) Environmental Policy Integrated Climate	RUE, TE	flexible N application rates (N-stress free days in 90% of crop growing period to an upper application limit of 200 kg ha-1) Constant P application rates.	annual adjustment of planting dates; total heat units to reach maturity remain constant no adjustment of cultivars	present day potential yields
GEPIC (Liu et al., 2009; Williams et al., 1989) GIS-based agroecosystem model integrating a bio-physical EPIC model (Environmental Policy Integrated Climate) with a Geographic Information System (GIS)	RUE, TE	flexible N application based on N stress >10% (limitation of potential biomass increase due to N stress) up to an upper national application limit according to FertiStat, fixed present day P application rates following FAO FertiStat database (2010)(Anon, n.d.)	decadal adjustment of planting dates, total heat units to reach maturity remain constant Adjustment of winter and spring wheat sowing areas based on temperature	present day yields

GAEZ-IMAGE (Leemans and Solomon, 1993) (called IMAGE in the main text) Integrated Model to Assess the Global Environment	LLP	Soil nutrient limiting factors are not accounted for	Adjustment of planting dates, total heat units to reach maturity remain constant Adjustment of summer and winter varieties in case of wheat and maize	present day yields
LPJ-GUESS	LLP, CC	Soil nutrient limiting factors are not accounted for	Adjustment of planting dates and total heat units to reach maturity Decadal adjustment of crop cultivar to give appropriate maturity dates (Lindeskog et al., 2013)	potential yields
LPJmL (Bondeau et al., 2007)	LLP, CC	Soil nutrient limiting factors are not accounted for	Fixed sowing dates (Waha et al., 2012), total heat units to reach maturity remain constant	present day yields (Fader et al., 2010)
PEGASUS (Deryng et al., 2011) Predicting Ecosystem Goods And Services Using Scenarios	RUE, TE	Fixed N, P, K application rates (IFA national statistics)	adjustment of planting dates, variable heat units to reach maturity	present day yields
pDSSAT	RUE, LLP, CC	Fixed N present day application rates	No adjustment of planting dates, total heat units to reach maturity	present day yields

			remain constant	

Table S1: Basic crop model characteristics with respect to the implementation of CO2 fertilization effect (as affecting 1) radiation use efficiency (RUE), 2) transpiration efficiency (TE), 3) leaf level photosynthesis (LLP), 4) canopy conductance (CC)), the accounting for nutrient constraints with respect to the CO2 fertilization effect, the assumption with respect to fertilizer application (N = nitrogen, P = Phosphorus, K = Potassium), implemented adaptation measures, and starting conditions.

2 Relative change in global production per global warming

2.1 Scenario Independence

The following plots show the global productions values for the four high priority crops under different management assumptions (unlimited irrigation, no irrigation and current irrigation) and CO2 concentrations ("noCO2" = based on fixed historical CO2 levels not accounting for the positive effect on crop production based on increasing CO2 (see caption of Figure S6 for the crop model specific levels of CO2); "CO2" = CO2 concentrations follow the historical evolution and the Representative Concentration Pathways (RCPs) afterwards.) The Figures show a relative close relationship between global productions and global mean warming. The relationship is only weakly dependent of the emissions scenarios.

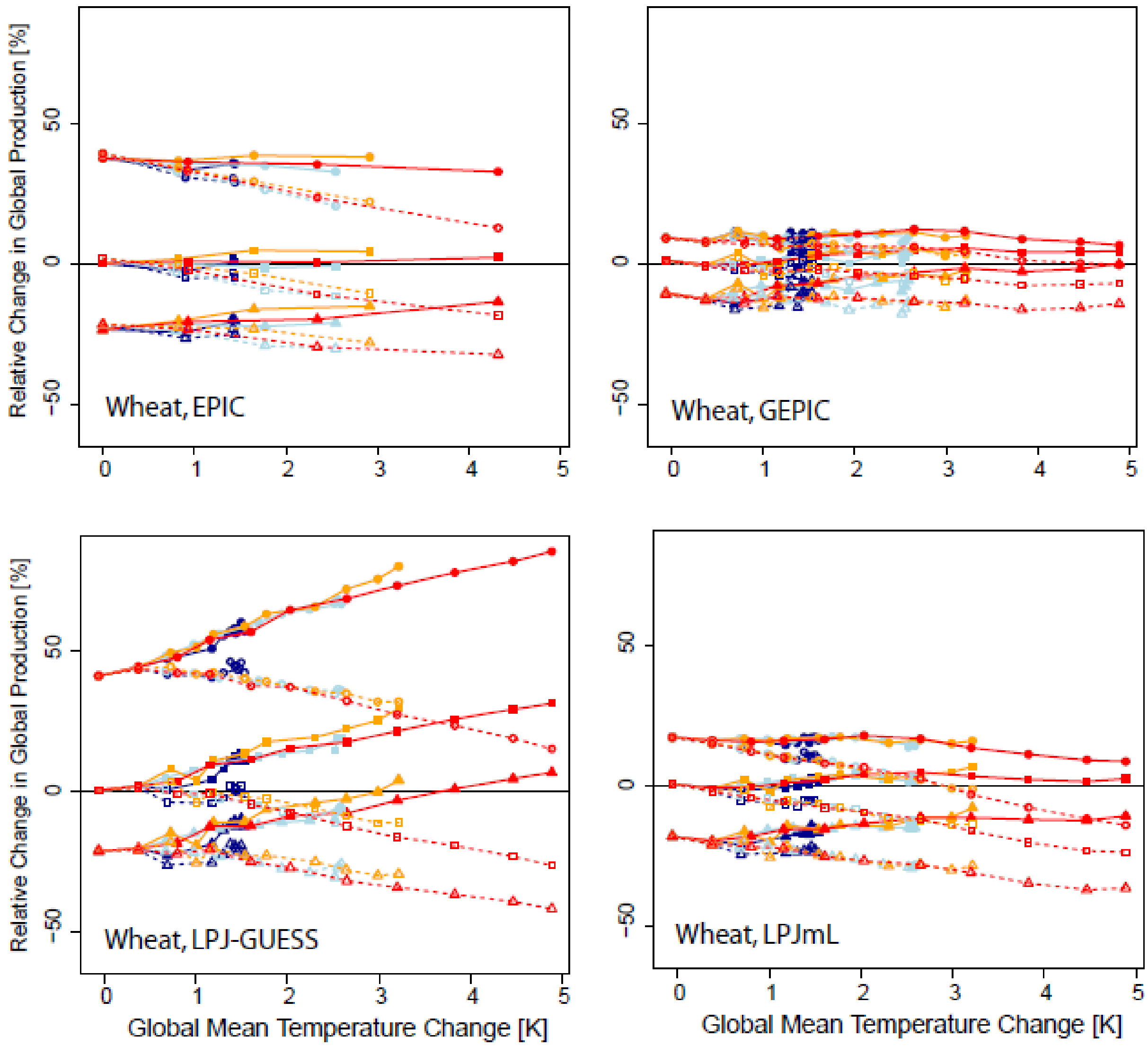
Wheat, EPIC
Wheat, GEPIC
Wheat, LPJ-GUESS
Wheat, LPJmL
Relative Change in Global Production [%]
Global Mean Temperature Change [K]
50
0
-50
0
1
2
3
4
5

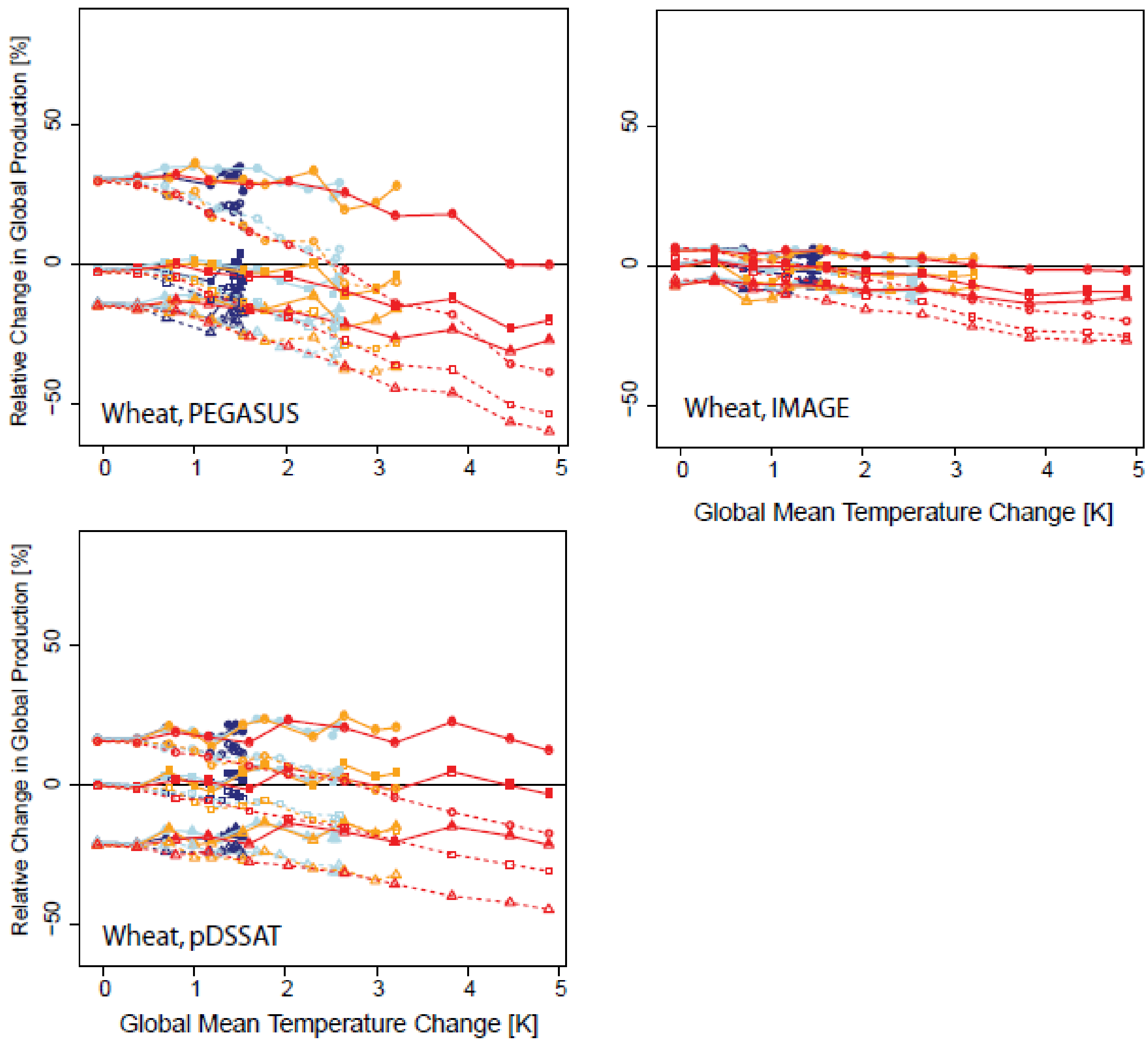

Figure S1: Relative changes in global wheat production with respect to the 1980-2010 reference period. Reference values are based on the “current irrigation + CO2” runs and identical for all considered management and CO2 scenarios. Color coding: Climate scenarios (red = RCP8.5, orange = RCP6.0, light blue = RCP4.5, dark blue = RCP2.6). Symbols: irrigation scenarios (dots = unlimited irrigation on the present day harvested area for wheat (MIRCA), squares = unlimited irrigation on the currently irrigated wheat area (MIRCA), triangles = global productions assuming no irrigation on the present day area used for wheat). Dashed lines represent the noCO2 runs while solid lines are based on the associated RCP-CO2 data.

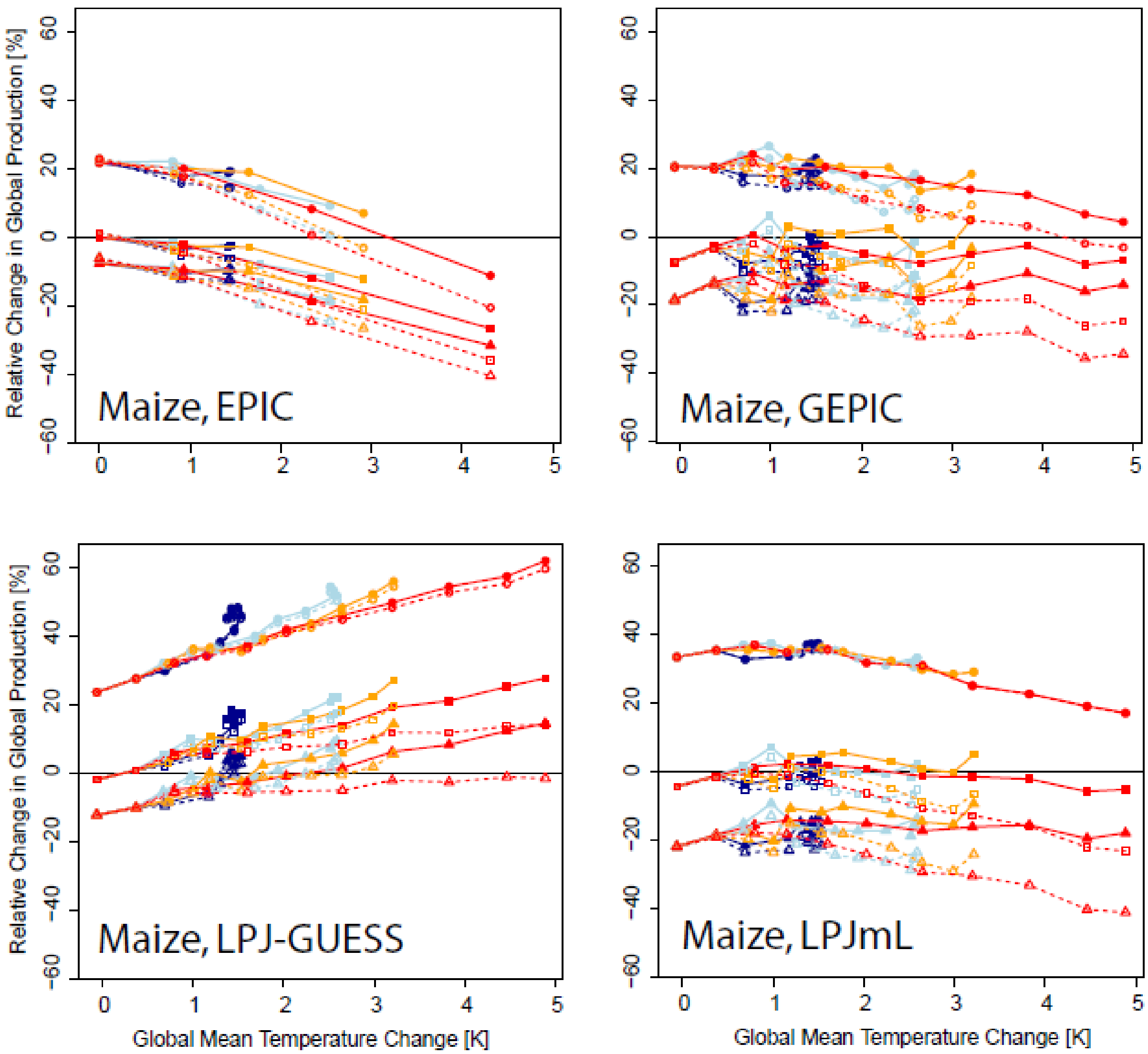
Maize, EPIC
Maize, GEPIC
Maize, LPJ-GUESS
Maize, LPJmL
Relative Change in Global Production [%]
Global Mean Temperature Change [K]

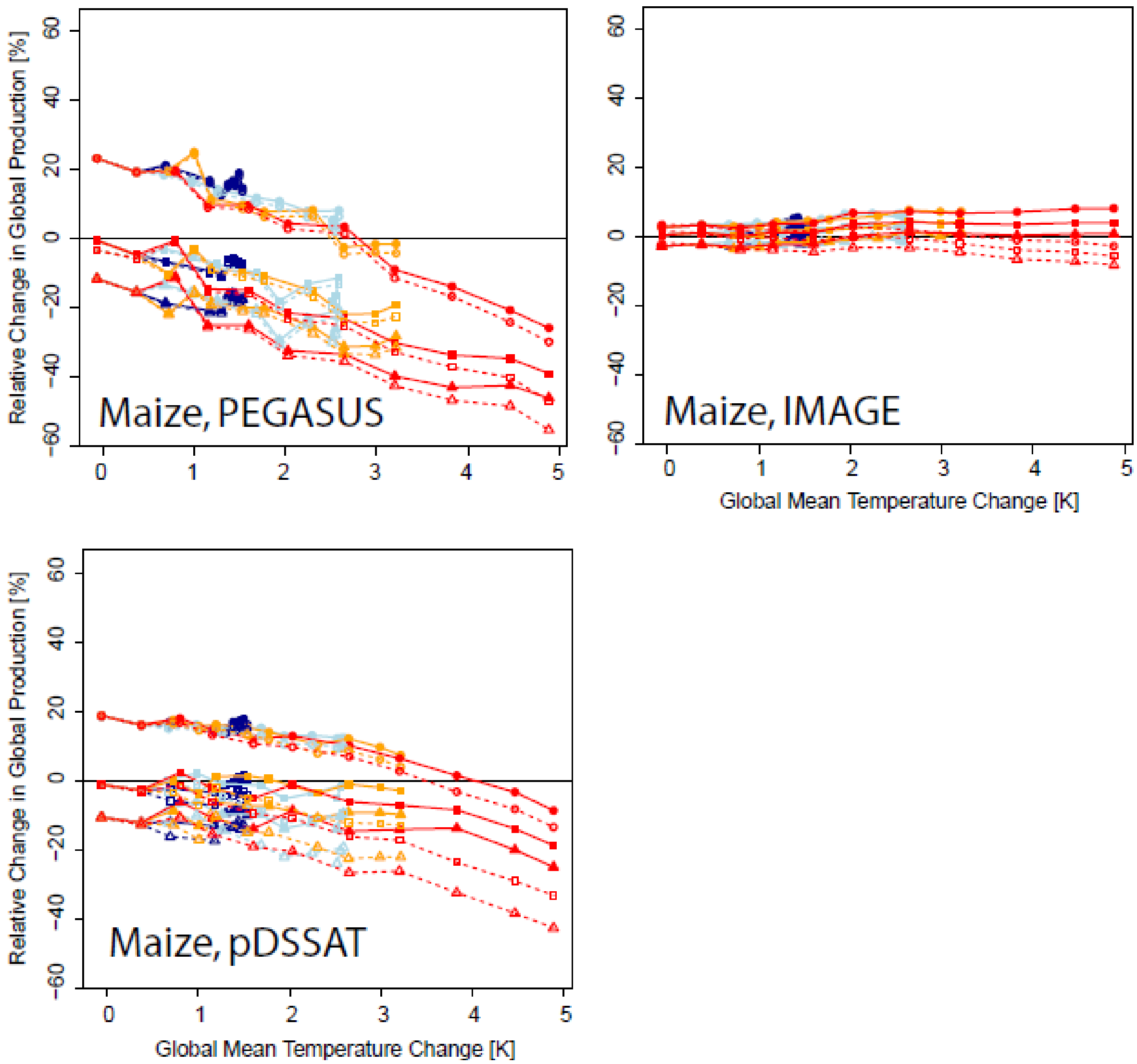

Figure S2: Relative changes in global maize production with respect to the 1980-2010 reference period. Reference values are based on the “current irrigation + CO2” runs and identical for all considered management and CO2 scenarios. Color coding: Climate scenarios (red = RCP8.5, orange = RCP6.0, light blue = RCP4.5, dark blue = RCP2.6). Symbols: irrigation scenarios (dots = unlimited irrigation on the present day harvested area for maize (MIRCA), squares = unlimited irrigation on the currently irrigated maize area (MIRCA), triangles = global productions assuming no irrigation on the present day area used for maize). Dashed lines represent the noCO2 runs while solid lines are based on the associated RCP-CO2 data.

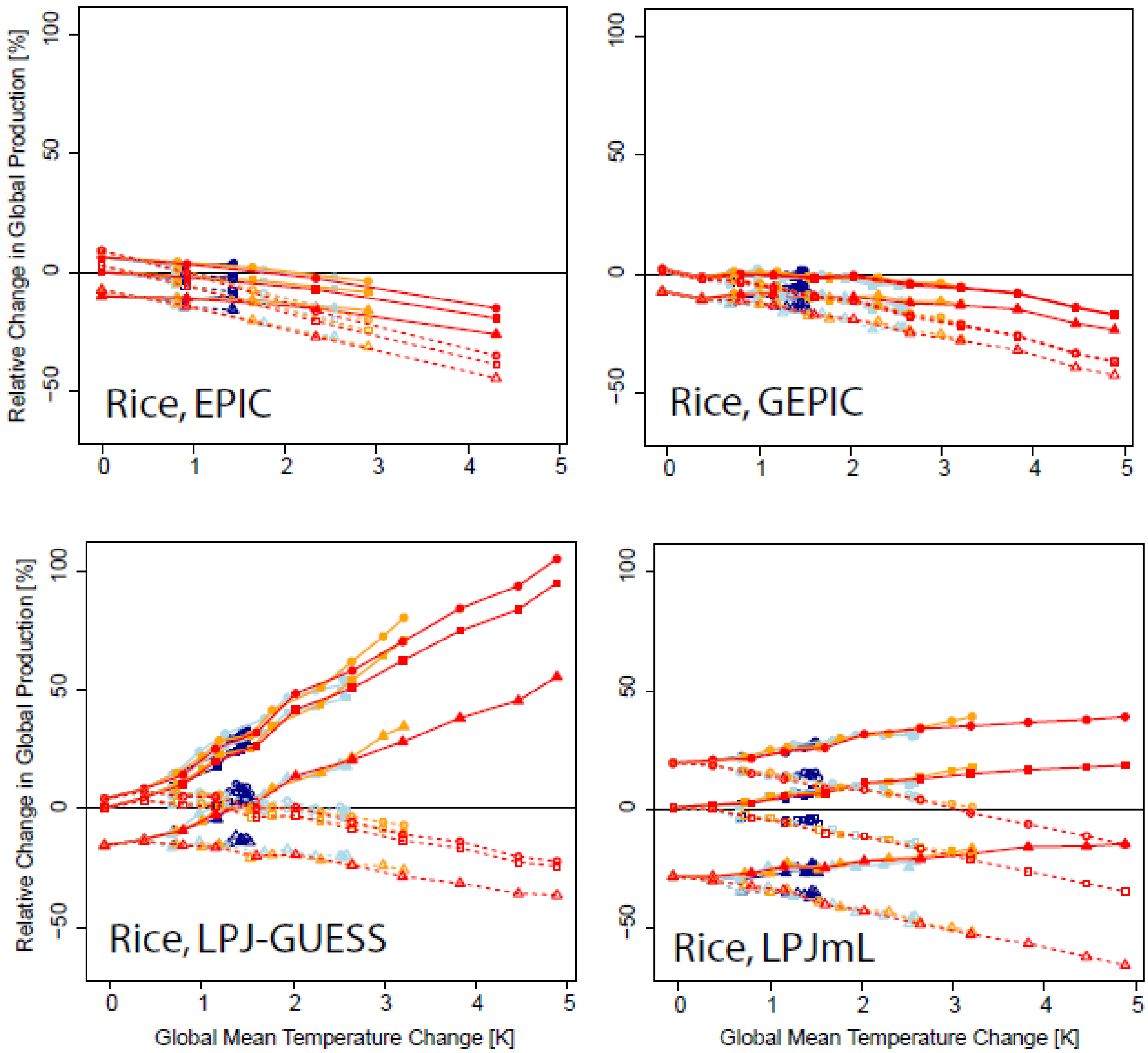

Figure S3: Relative changes in global rice production with respect to the 1980-2010 reference period. Reference values are based on the “current irrigation + CO2” runs and identical for all considered management and CO2 scenarios. Color coding: Climate scenarios (red = RCP8.5, orange = RCP6.0, light blue = RCP4.5, dark blue = RCP2.6). Symbols: irrigation scenarios (dots = unlimited irrigation on the present day area used for rice (MIRCA), squares = unlimited irrigation on the currently irrigated rice area (MIRCA), triangles = global productions assuming no irrigation on the present day area used for rice). Dashed lines represent the noCO2 runs while solid lines are based on the associated RCP-CO2 data.

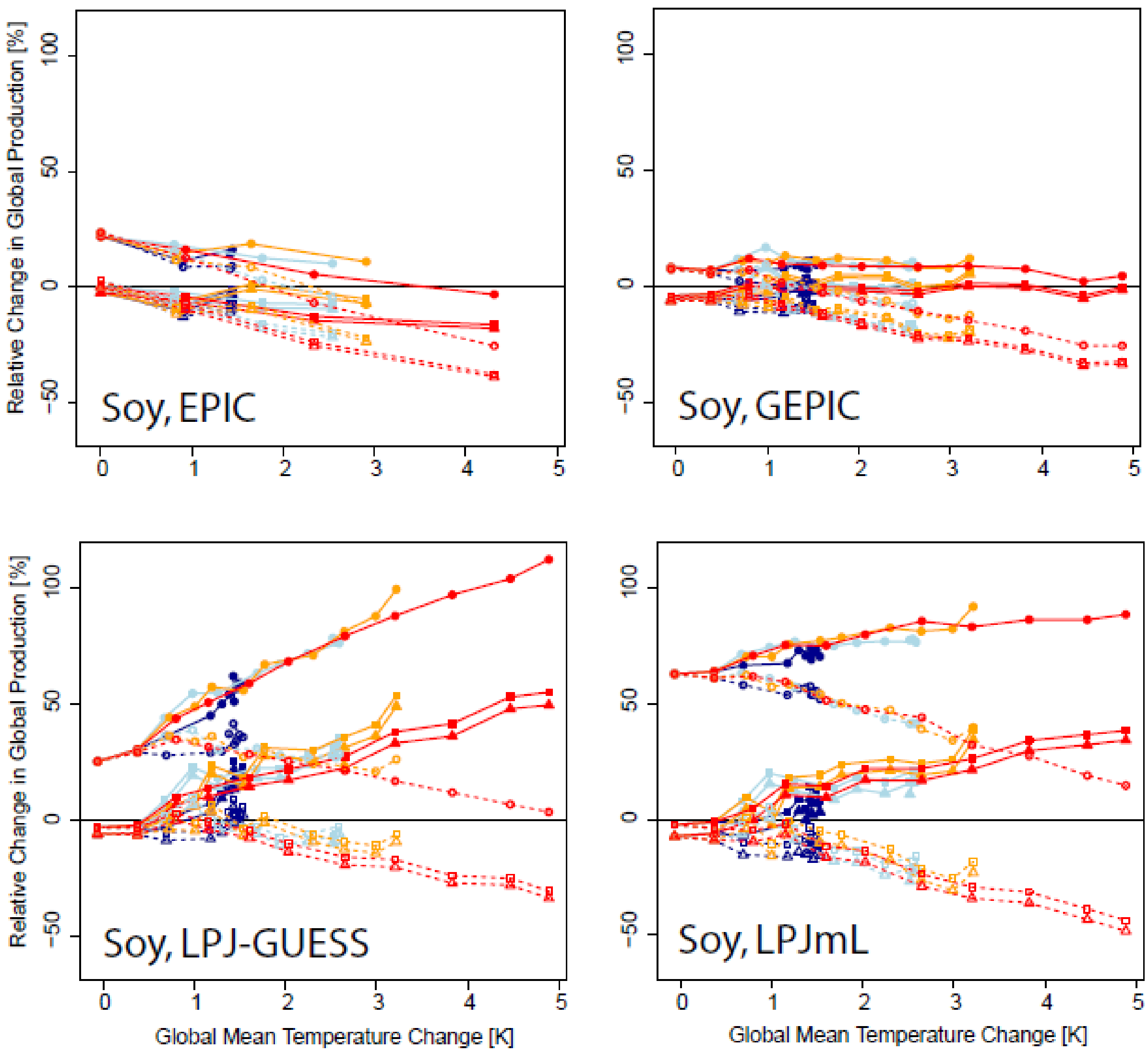
Soy, EPIC
Soy, GEPIC
Soy, LPJ-GUESS
Soy, LPJmL
Relative Change in Global Production [%]
Global Mean Temperature Change [K]

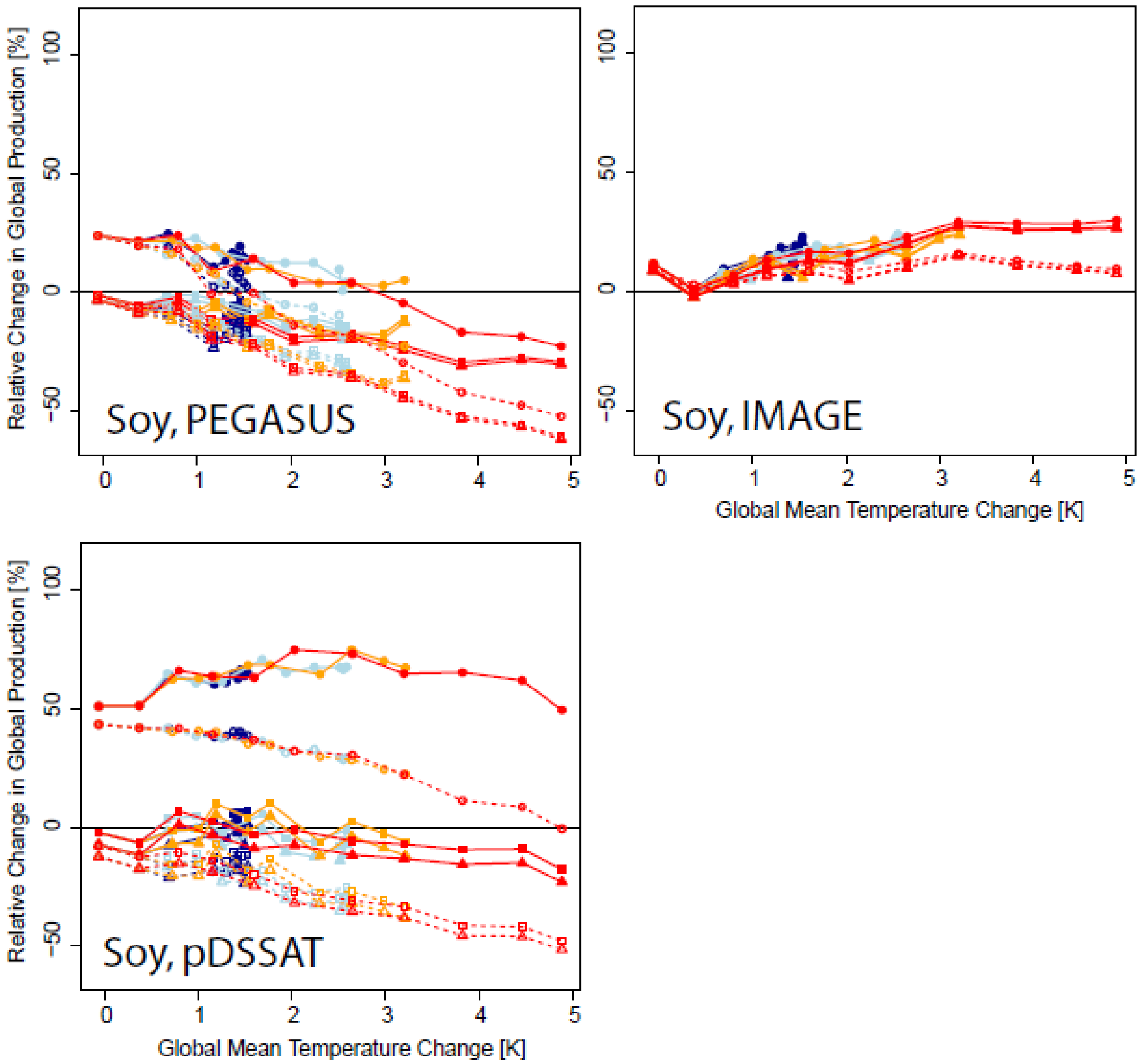

Figure S4: Relative changes in global soy production with respect to the 1980-2010 reference period. Reference values are based on the "current irrigation + CO_2" runs and identical for all considered management and CO_2 scenarios. Color coding: Climate scenarios (red = RCP8.5, orange = RCP6.0, light blue = RCP4.5, dark blue = RCP2.6). Symbols: irrigation scenarios (dots = unlimited irrigation on the present day area used for soy (MIRCA), squares = unlimited irrigation on the currently irrigated soy area (MIRCA), triangles = global productions assuming no irrigation on the present day area used for soy). Dashed lines represent the noCO_2 runs while solid lines are based on the associated RCP-CO_2 data.

2.2 Trend in global production in terms of global mean warming

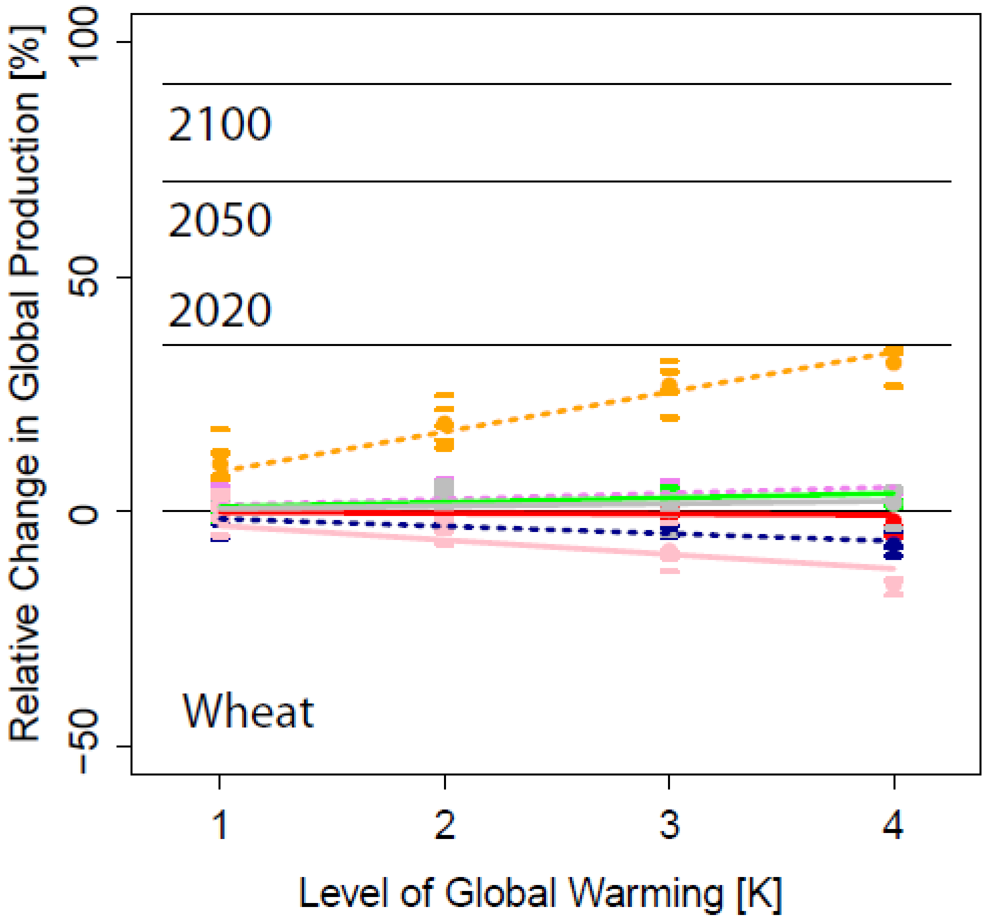

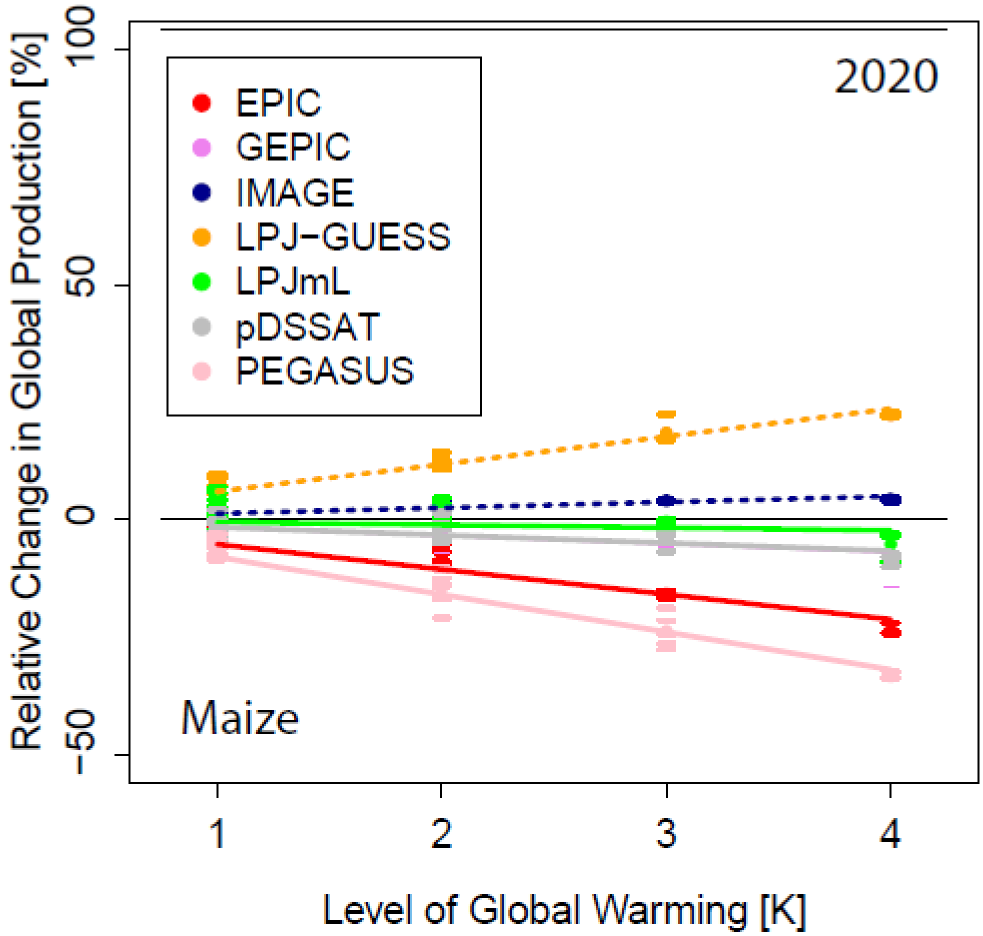
2020
EPIC
GEPIC
IMAGE
LPJ−GUESS
LPJmL
pDSSAT
PEGASUS
Maize
Relative Change in Global Production [%]
100
50
0
−50
1
2
3
4
Level of Global Warming [K]

1

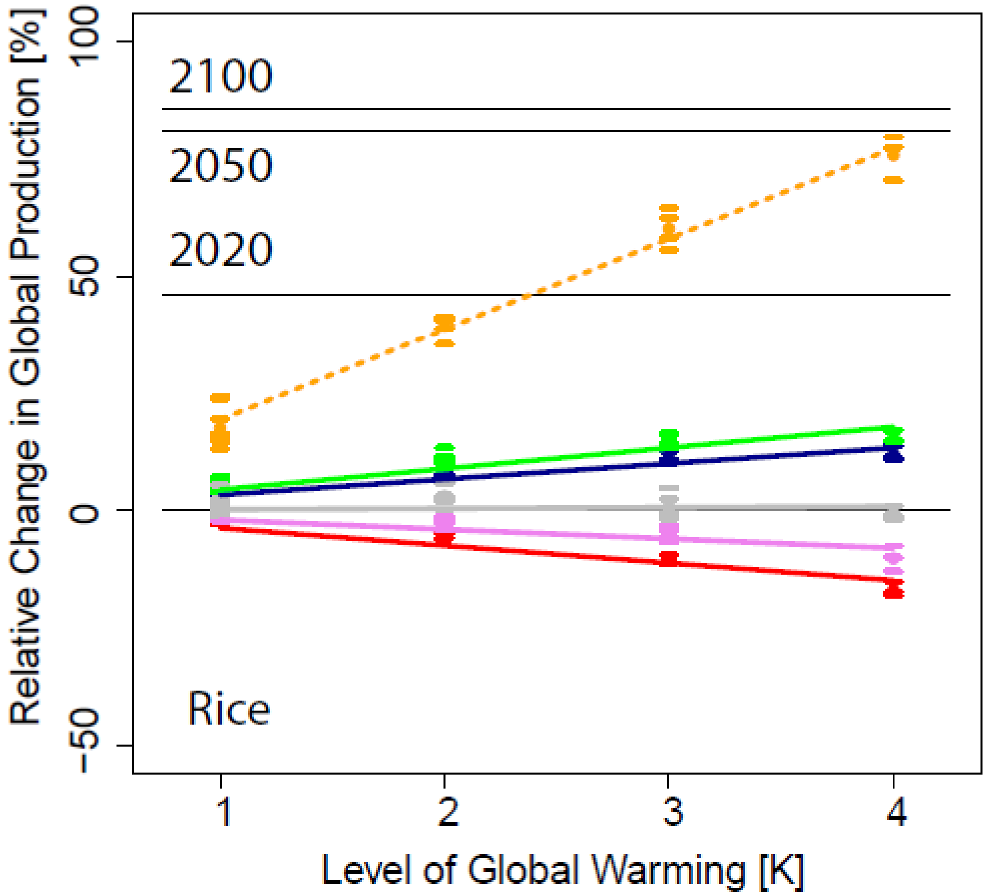
2100
2050
2020
Rice
100
50
0
−50
1
2
3
4
Relative Change in Global Production [%]
Level of Global Warming [K]

1

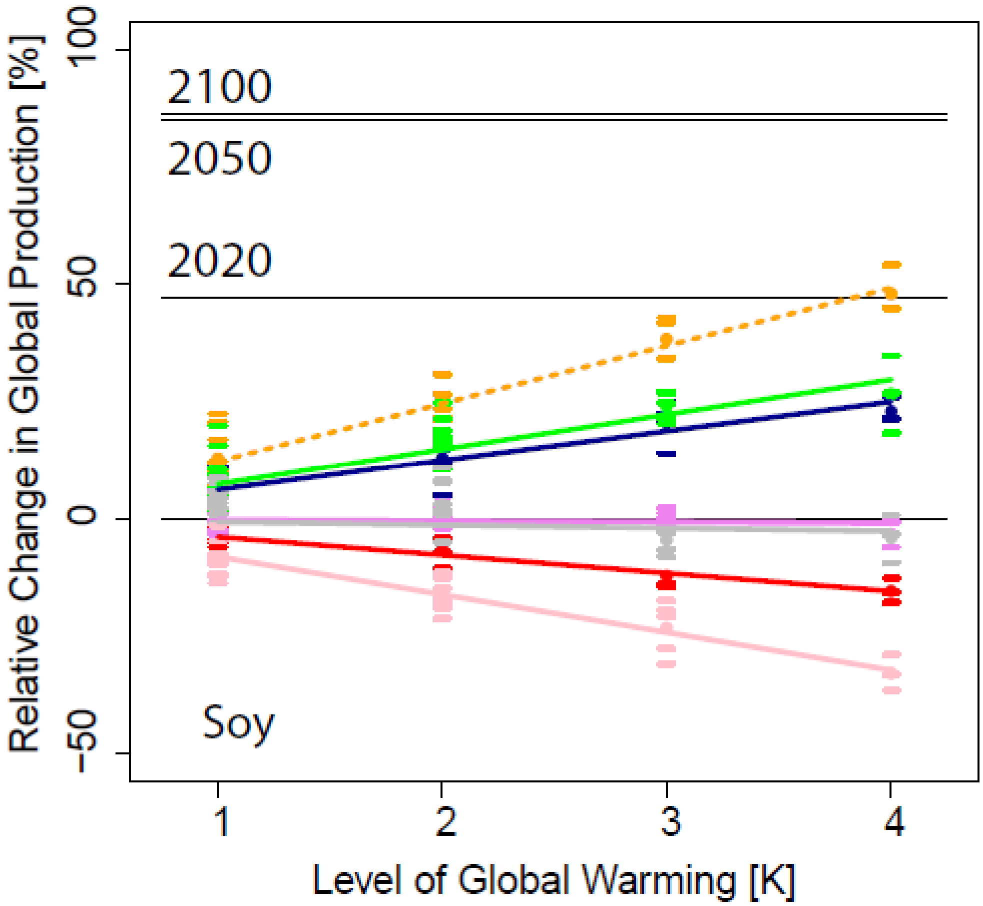

Figure S5: Individual bars and dots are identical to the elements of the first column of each global mean warming bin shown in Figure 3 of the main text except for the linear trend lines included here. They are based on a linear regression based on the four crop model specific mean values (colored dots at each level of global warming) and forced through zero. The associated slopes are reported in Table S2.

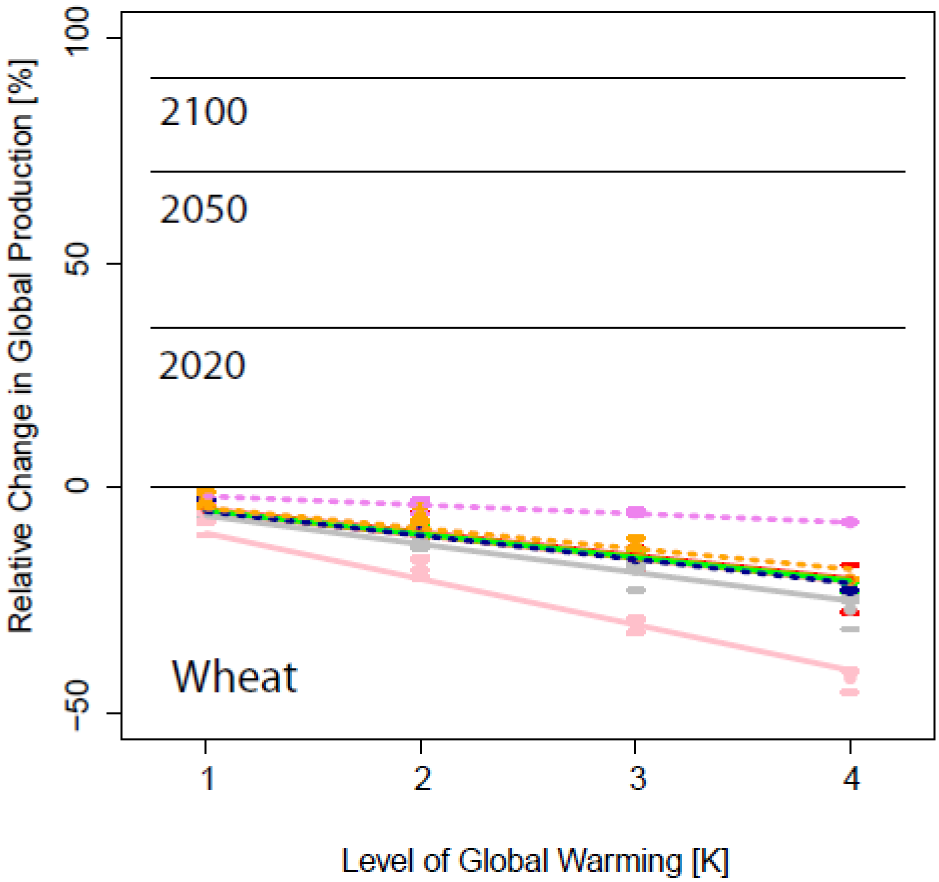
Relative Change in Global Production [%]
100
50
0
−50
2100
2050
2020
Wheat
1
2
3
4
Level of Global Warming [K]

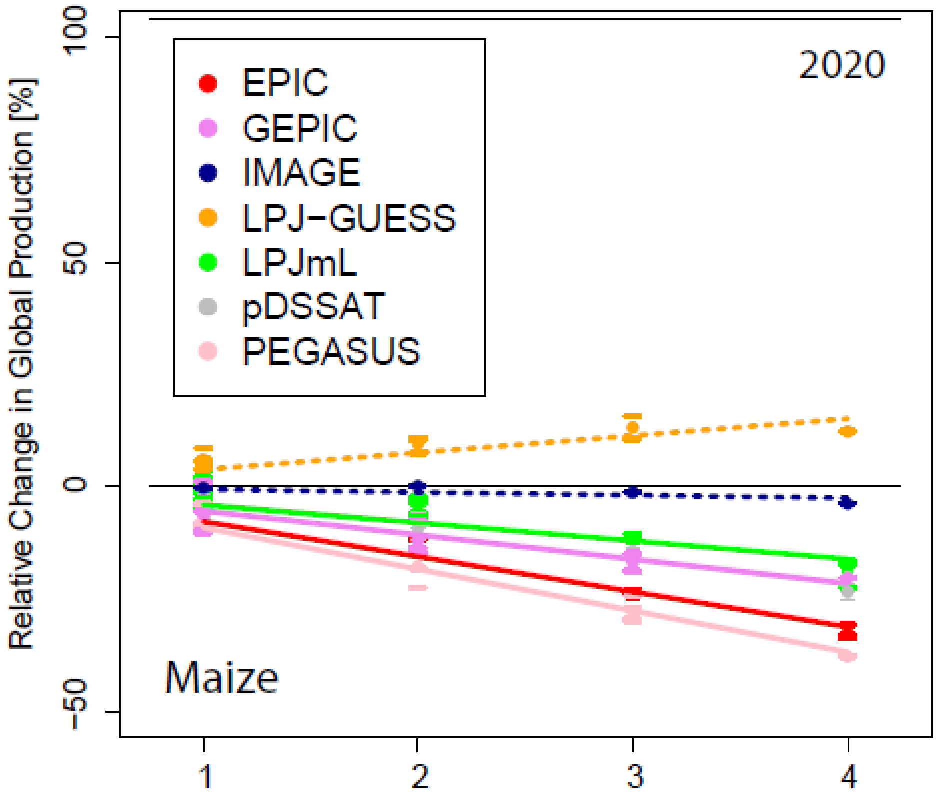

2020
EPIC
GEPIC
IMAGE
LPJ−GUESS
LPJmL
pDSSAT
PEGASUS
Maize
Relative Change in Global Production [%]
100
50
0
−50
1
2
3
4

1

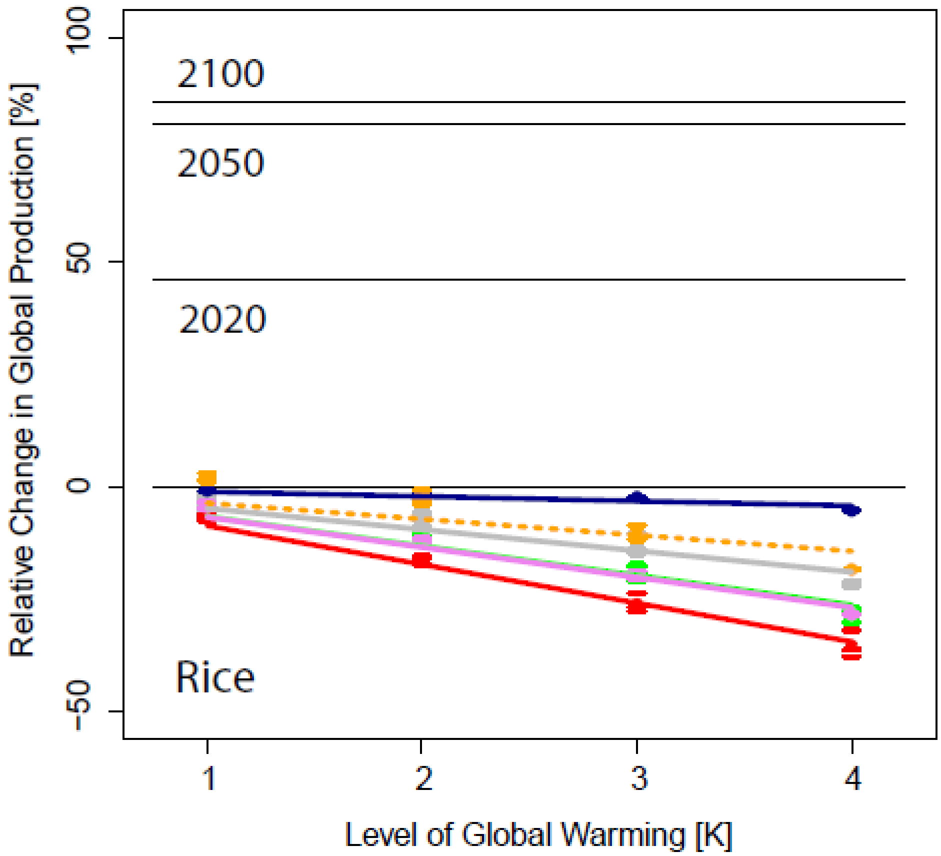

2100
2050
2020
Rice
100
50
0
-50
1
2
3
4
Relative Change in Global Production [%]
Level of Global Warming [K]

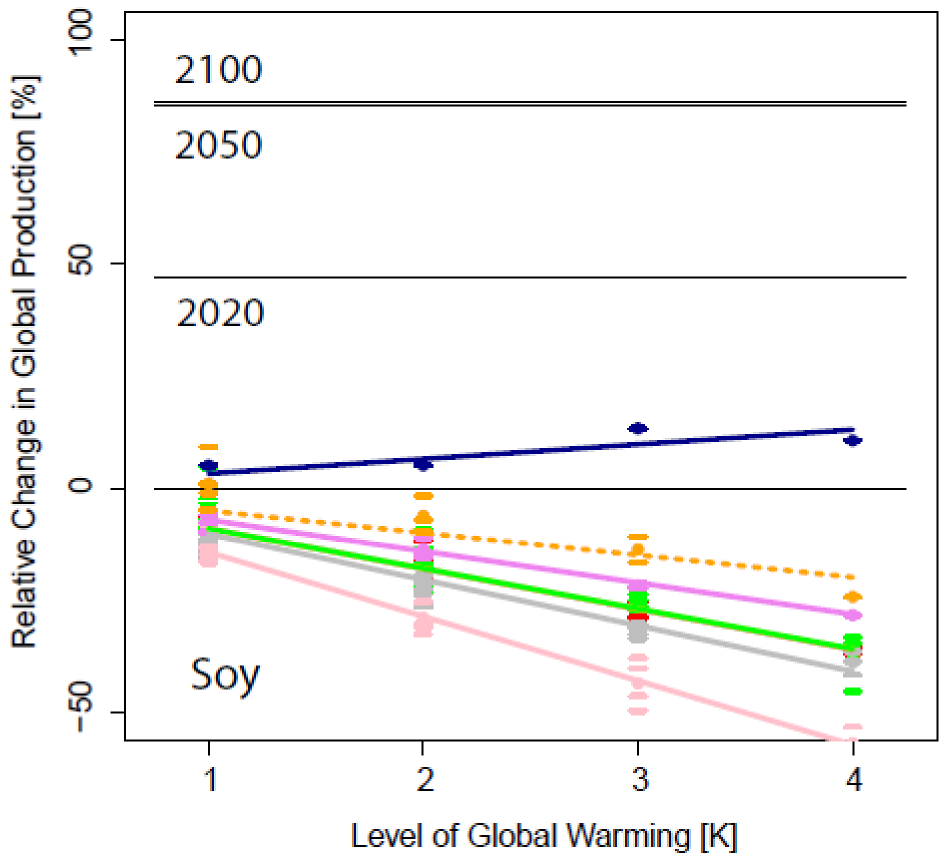

Figure S6: Analogous to Figure S5 but based on the available " constant CO2" runs for the HadGEM2, IPSL, and MIROC model reaching 4 K of warming in comparison to the 1980-2010 reference value. Fixed CO2 levels for constant CO2 runs: 380 ppm (year 2005) for EPIC, 364 ppm (year 2000) for GEPIC, 369 ppm (year 2000) for IMAGE; 379 ppm (year 2005) for LPJ-GUESS; 370 ppm (year 2000) for LPJmL; 369 ppm (year 2000) for PEGASUS; 330 ppm (year 1975) for pDSSAT. The slopes of the regression lines are reported in Table S2.

	Wheat (ΔP/ΔT) [%/K]		Maize (ΔP/ΔT) [%/K]		Rice (ΔP/ΔT) [%/K]		Soy (ΔP/ΔT) [%/K]	
	↑	→	↑	→	↑	→	↑	→
EPIC	-0.19	-5.15	-5.32	-7.82	-3.73	-8.60	-3.85	-8.98
GEPIC	1.31	-1.94	-1.71	-5.41	-2.05	-6.69	-0.23	-7.03
IMAGE	-1.57	-5.33	1.22	-0.65	3.34	-1.04	6.27	3.26
LPJ-GUESS	7.48	-4.54	5.90	3.77	19.35	-3.56	12.31	-4.97
LPJmL	0.96	-5.18	-0.59	-4.05	4.45	-6.55	7.44	-8.96
pDSSAT	0.56	-6.30	-1.68	-5.36	0.22	-4.72	-0.66	-10.21
PEGASUS	-3.05	-10.16	-8.00	-9.23			-8.04	-14.30
median	0.56	-5.18	-1.68	-5.36	1.78	-5.64	-0.23	-8.96
mean	0.78	-5.51	-1.47	-4.11	3.60	-5.19	1.89	-7.13
stdev	3.33	2.45	4.47	4.42	8.32	2.68	7.08	5.48
stdev CO2 effect	2.92		0.98		7.36		5.58	

Table S2: Relative change in global crop production [%/K] assuming fixed present day harvested areas and unlimited irrigation on the reported irrigated land (Portmann et al., 2010). Results are listed for the model runs accounting for the CO2 fertilization effect under changing CO2 concentration corresponding to the RCP scenarios (↑) and fixed CO2 concentrations (→).

3 Calculation global crop production under additional irrigation accounting for water constraints

3.1 Available water for irrigation

Approximation of the overall amount of water available in a Food Production Unit (FPU)

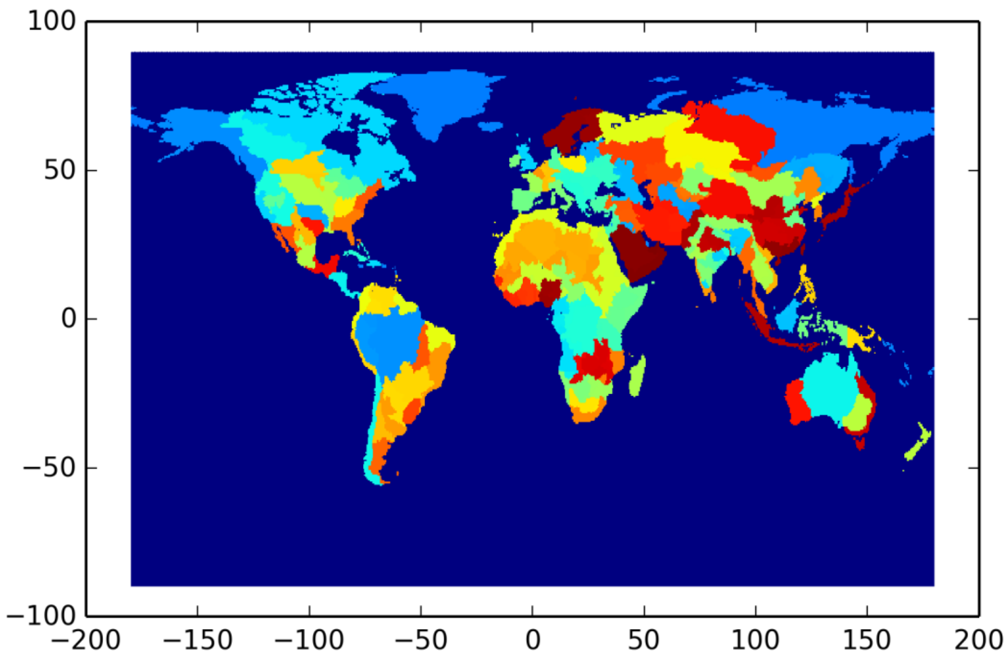

Figure S7: Map of Food Production Units (FPUs) (Kummu et al., 2010).

To estimate the amount of water available for irrigation within each FPU we use the sum of surface and sub-surface runoff provided by the different ISI-MIP water models (see Table S3 for their basic characteristics). This means that the "available irrigation water" used within our study only includes renewable surface and groundwater but not groundwater that could be withdrawn in excess of groundwater recharge (thus leading to groundwater depletion). Part of the irrigation water available within an FPU might not be generated within the same FPU but transported from an upstream FPU. The spatially aggregated runoff only represents a proxy for the irrigation water "generated" in the associated FPU. To also account for the transported water we proceed in the following way:

1. The overall amount of water generated within a river basin (aggregated runoff) is re-distributed within the same river basin according to the discharge values. In this way the overall amount of water does not change but is “concentrated” in the rivers.

2. The re-distributed runoff is afterwards aggregated over the FPUs that might only cover part of the river basins.

Runoff (qtot [kg/m2/s]) and discharge (dis [kg/m2/s]) are provided on a monthly or daily resolution by all participating hydrological models. They are annually averaged before re-distribution as the irrigation water requirements (pirrww) estimated by the crop models are also only reported on an annual basis.

The “irrigation water” required for full irrigation is usually provided by the crop models as the overall amount of irrigation water applied to the harvested crops and reported for the harvesting year. It might be partly used in the previous year if the planting day falls in that year. Therefore we used a two year running mean of the “available water” (calculated as described above) to estimated the available water relevant for the reported yields. For all crop models reporting pirrww in the harvesting year the two year average is taken over the actual and the previous year. For pDSSAT we use the average over the actual and the following year as pirrww is reported in the planting year.

Calculation of the crop specific amount of available irrigation water

To calculate the crop specific available irrigation water we have to take into account that not all of the “available water” can be used for irrigation and that part of the water spent for irrigation will be used for other crops not covered by the four main ISI-MIP crops. To account for both effects we proceed in the following way:

The maximum available irrigation water for one specific high priority crop is assumed to be a fraction of the “available” water taking into account the area used for the specific crop and the amount of water needed for its full irrigation. The division is done according to the following assumptions:

1) 40% of the overall runoff can be used for irrigation or other purposes. The 40% availability constraint follows (Gerten et al., 2011) and attempts to account for the various limitations that reduce utilization of water resources for irrigation: spatial and temporal disagreement between water requirements for crops and water availability in rivers, lakes, and aquifers as well as losses due to transport, storage or inefficient application.

2) To estimate the amount that is actually available for irrigation the amount of water used for manufactoring and electricity productions (amanww) as well as domestic withdrawal

(adomww) provided by H08 is subtracted from the "40% budget". Irrigation water withdrawals from currently irrigated lands (airrww) are not subtracted as the starting point in this analysis is the rainfed-only situation.

3) 60% of the remaining amount is assumed to be directly available to the plants[1]. It is split up between the high priority crops and the other crops planted within the considered FPU based on LPJmL simulations:

Assuming full irrigation on current harvesting areas (Portmann et al., 2010), crop specific pirrww data were spatially aggregated within each FPU and averaged over the reference period (1980-2010). For the crops included in the MICRA data set but not covered by LPJmL simulations we used a) median, b) maximum and c) minimum irrigation values calculated at each grid point over all crops and managed grass land simulated by LPJmL. In the case of the MIRCA data set the simulated crops are wheat, rice, maize, soybeans, cassava, millet, peanuts, pulses, rapeseed, sugar beet, sugar cane and sunflowers. Not covered crops are barley, rye, sorghum, potatoes, oil palm, citrus, date palm, vine, cotton, cocoa, coffee, "other perennial" and "other annual crops".

In the minimal and median irrigation setting we assume that managed grass land is not irrigated at all (which means that more water is available for the four crops considered in this paper following the reasoning of an optimistic scenario).

The LPJmL specific fraction of the aggregated pirrww data associated with the high priority crops is then assumed for all crop models providing simulations of the four high priority crops. PEGASUS is excluded from this experiment as it does not provide rice data.

3) The split-up of irrigation water within the group of the high priority crops is determined in a similar way as described above. However in the case we used crop model specific values based on the aggregated pirrww data of the full irrigation runs (assuming MIRCA current land use) of the high priority crops.

3.2 Optimal Distribution of the "available water"

Within the paper "optimal distribution of water" within one FPU means a distribution according to the highest water use efficiency defined at each grid cell as yield increase per applied irrigation water. Starting from the grid cell with the highest water use efficiency the water assigned for irrigation of each crop is used to fully irrigate as much area of the respective crop in the considered FPU as possible. If the water is not sufficient to irrigate the whole crop area in

[1] The irrigation water demand reported as „pirrww" by the crop models partly includes assumptions about the efficiency of irrigation, i.e. pirrww is higher than the water assumed to be directly available to the plants. Here, the associated pirrww values are harmonized assuming a homogeneous project efficiency of 60%.

a cell the irrigated area is reduced accordingly and the remaining area in that cell and in all cells with lower water productivity is assumed to be rainfed.

Calculation of "water use efficiency"

Yields and the amount of irrigation water applied are usually reported for the harvesting year except for pDSSAT where the information is written to the associated planting year. In most of the cases there is a one to one relationship between yield increases by optimal irrigation and the applied irrigation water as pirrww is reported as the overall amount of water required to generate the "full irrigation yields" no matter if part of the growing season lies in the previous calendar year. In these cases "water use efficiency" can be estimated on an annual basis by subtracting the no-irrigation yields from the full irrigation yields and dividing the difference by the pirrww value of the same year. That is different for LPJmL where the reported irrigation water is not directly associated with the generated yields but aggregated over the individual calendar years. Therefore the water actually needed to generate the full irrigation yields might be a mixture of the pirrww data of the harvesting year and the previous year. As a proxy for the "required irrigation water" we used the mean pirrww value of both years to calculate annual data of water use efficiency in case of LPJmL.

To account for the fact that irrigation measures have to be installed and will not change from year to year we use ten year averages (covering the actual and the 9 previous years) of the water use efficiency to distribute the water.

The scheme assumes that irrigation is always 'all or nothing' while realistically crop production could well be increased in water-limited FPUs by "deficit irrigation" in favor of larger irrigated areas, as the irrigation water use efficiency typically declines at higher irrigation levels (Fereres and Soriano, 2007).

3.3 Irrigation scheme for the LU change experiment

In this experiment we apply a land use pattern provided by the LPJmL + MAgPIE agro-economic simulation for the HadGEM2, RCP8.5 climate scenario and the SSP2 assumptions with respect to population and GDP. The agro-economic land use model MAgPIE is designed to provide demand fulfilling land use patterns in this case based on the biophysical input data delivered by LPJmL. The assumed demand of rice, wheat, maize and soy is identical to the demand data used in the main text.

While within MAgPIE it is assumed that there is technological progress increasing crop yields we only use the land use information and do not assume changes in other management options. The irrigations scheme follows the above procedure based on the optimal distribution of the crop specific available irrigation water.

In this exercise we estimate the additional effect of land use changes and estimate the remaining adaptive pressure that might be met by other management options not covered by the ISI-MIP simulations.

The calculation of the crop specific amount of available irrigation water is analog to the procedure described for the MIRCA data set. However, for MAgPIE the simulated crops are cassava, managed grass, peanuts, maize, pulses, rapeseed, rice, soybeans, sugar beet, sugar cane, sunflowers, millet and wheat. The following crops are considered as “not simulated”: bioenergy grass, bioenergy tree, cotton, oil palm, potatoes, and “others”.

3.4 Calculation of global production under additional irrigation for crop models that do not provide the full information to apply the above water distribution scheme

PEGASUS and GAEZ-IMAGE provide full irrigation and no irrigation yields but not the complete information necessary to apply the above water distribution scheme. In order to not lose the available information about $P_{unlimited}$ (global production under unlimited irrigation) and P_R (rainfed global production) the production under water constraints $(P_{limited})_{ij}$ is calculated as $(P_{limited})_{ij}$ = - $(P_R)_i$ + α_j * $((P_{unlimit})_i$ - $(PR)_i)$, where α_j is the water model specific mean over all production fractions α_{kj} calculated for each crop model k where the full information is available.

3.5 Participating hydrological models

Model name	Energy balance	Evaporation scheme	Runoff scheme	Snow scheme	Vegetation dynamics	CO_2 effect
DBH (Tang et al., 2007, 2008)	Yes	Energy balance	Infiltration excess	Energy balance	No	Constant
H08 (Hanasaki et al., 2008; Hanasaki, N., Kanae, S., Oki, T., Masuda, K., Motoya, K., Shirakawa	Yes	Bulk formula	Saturation excess, non-linear	Energy balance	No	No

and Shen, Y., and Tanaka, 2008)						
JULES (Best et al., 2011; Clark et al., 2011)	Yes	Penman-Monteith	Infiltration excess, saturation excess, groundwater.	Energy balance	Yes	Yes
LPJmL (Bondeau et al., 2007; Rost et al., 2008)	No	Priestley-Taylor	Saturation excess	Degree-day	Yes	yes
Mac-PDM.09 (Arnell, 1999; Gosling and Arnell, 2011)	No	Penman-Monteith	Saturation excess, non-linear	Degree-day	No	No
MATSIRO (Pokhrel et al., 2012; Takata et al., 2003)	Yes	Bulk formula	Infiltration excess, saturation excess, groundwater.	Energy balance	No	Constant
MPI-HM (Hagemann and Gates, 2003; Stacke and Hagemann, 2012)	No	Penman-Monteith	Saturation excess, non-linear	Degree-day	No	No
PCR-GLOBWB (Van Beek et al., 2011; Wada et al., 2010)	No	Hamon	Saturation Excess Beta Function	Degree Day	No	No
VIC (Liang	Only	Penman-	Saturation	Energy	No	No

and Lettenmaier, 1994; Lohmann et al., 1998)	for snow.	Monteith	excess, non-linear	balance.		
WaterGAP (Döll et al., 2003, 2012; Flörke et al., 2012)	No	Priestley-Taylor	Beta function	Degree day	No	No
WBM (Vörösmarty et al., 1998; Wisser et al., 2010)	No	Hamon	Saturation Excess	Empirical temp and precip based formula	No	No

Table S3: Basic water model characteristics and references. In case of the evapotranspiration scheme "Bulk formula" means that bulk transfer coefficients are used when calculating the turbulent heat fluxes. In case of the runoff scheme "beta function" means that runoff is a nonlinear function of soil moisture.

4 Production Fractions

To assess whether the increase in production under "additional irrigation" is mainly biophysically limited by potential yields under unlimited irrigation or by water availability we introduce the production fractions $\alpha_{ij} = ((P_{limited})_{ij} - (P_R)_i) / ((P_{unlimit})_i - (PR)_i)$, where $(P_{limited})_{ij}$ is the potential production accounting for water constraints (scenario discussed above), $(P_R)_i$ denotes rain-fed production, and $(P_{unlimit})_i$ is the potential production under full irrigation for each GGCM (i) and hydrological model (j). Cumulative distributions of α_{ij} for different levels of global warming (see Fig. S8) show that the uncertainty budget of the production fractions α differs from the one of projected production changes. The crop-model-induced spread of α (spread of light blue squares in Fig. S8 below) is comparable or smaller than the spread introduced by the different hydrological models (spread of dark blue triangles in Fig. S8). The GGCM contribution to the spread of α is caused by 1) differences in the absolute amount of water required to reach full irrigation, 2) differences in the determination of the crop-specific fractions of the overall amount of irrigation water (see SI), and 3) the production increase due to irrigation. The median α, based on the "additional irrigation" scenario, is about 60% in the case of wheat and about 80% for maize. In comparison, assuming unlimited irrigation on currently irrigated land the median production fraction for wheat over all GGCMs already reaches 50% at 1°C, 50% at 2°C, 40% at 3°C, and 30% at 4°C. Thus the benefit of additional irrigation is relatively small. In the case of maize the corresponding values are 30% at 1, 2, and 3°C and 40% at 4°C. Assuming unlimited irrigation on currently irrigated land the median production fraction for rice over all crop models already reaches about 75% at 1, 2, 3, and 4°C. For soy the value only reaches about 10% at all levels of global warming. In both cases median values under the "additional irrigation" scenario also reach about 80%. In the LU change scenario the production fraction reaches about 90% for all crops. Thus, the projected change in crop production is close to the maximum change assuming unlimited irrigation.

The distribution does not show a clear dependence on global warming. This could be due to 1) the high level of aggregation (though runoff decreases in many regions, it increases in others, Fig. 1 of (14)), 2) reduced water demand by reduced growing seasons lengths, and 3) decreasing water demand under CO_2 fertilization (20).

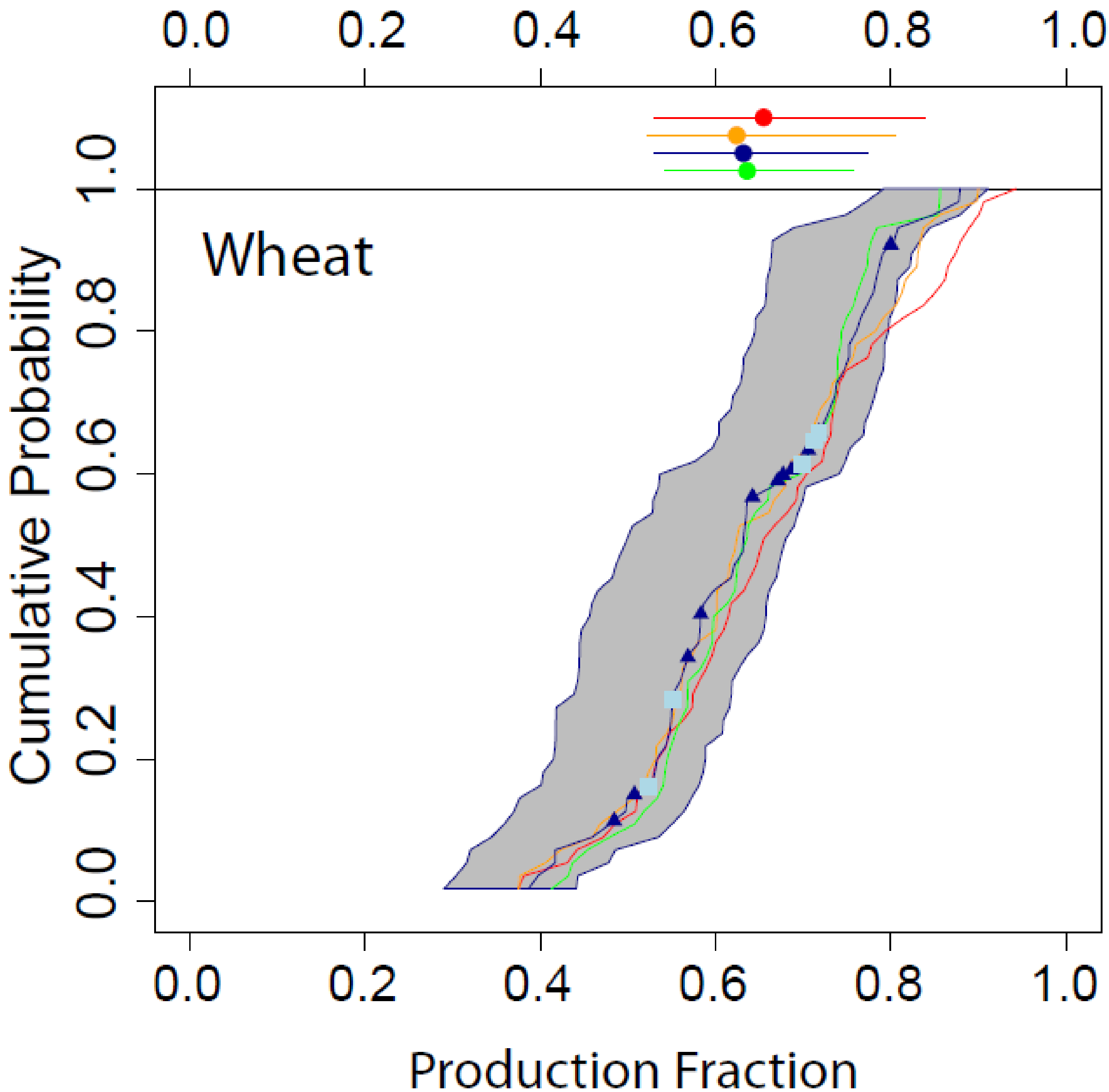

Wheat
Cumulative Probability
Production Fraction
0.0
0.2
0.4
0.6
0.8
1.0

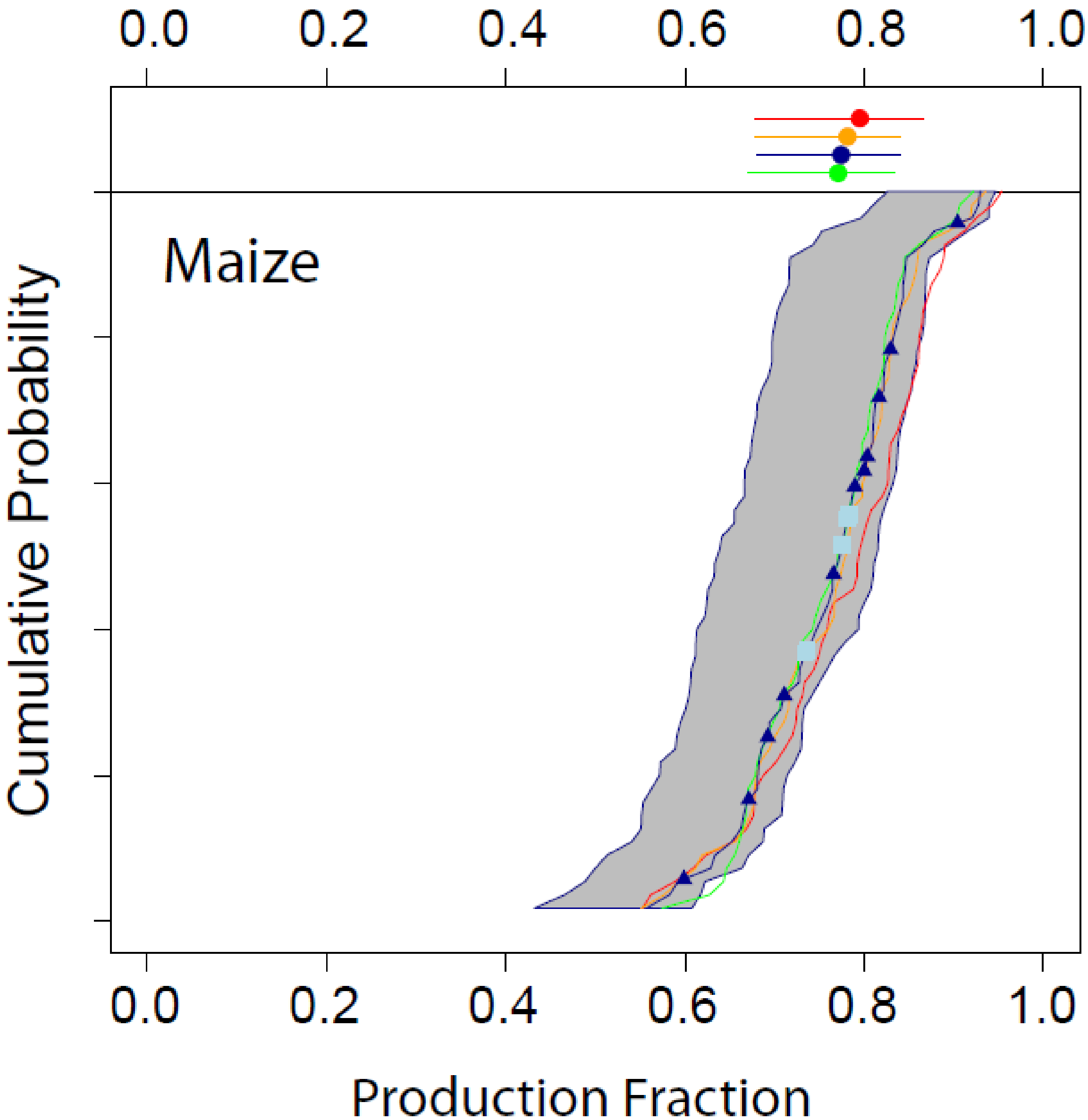
0.0
0.2
0.4
0.6
0.8
1.0
Maize
Cumulative Probability
Production Fraction

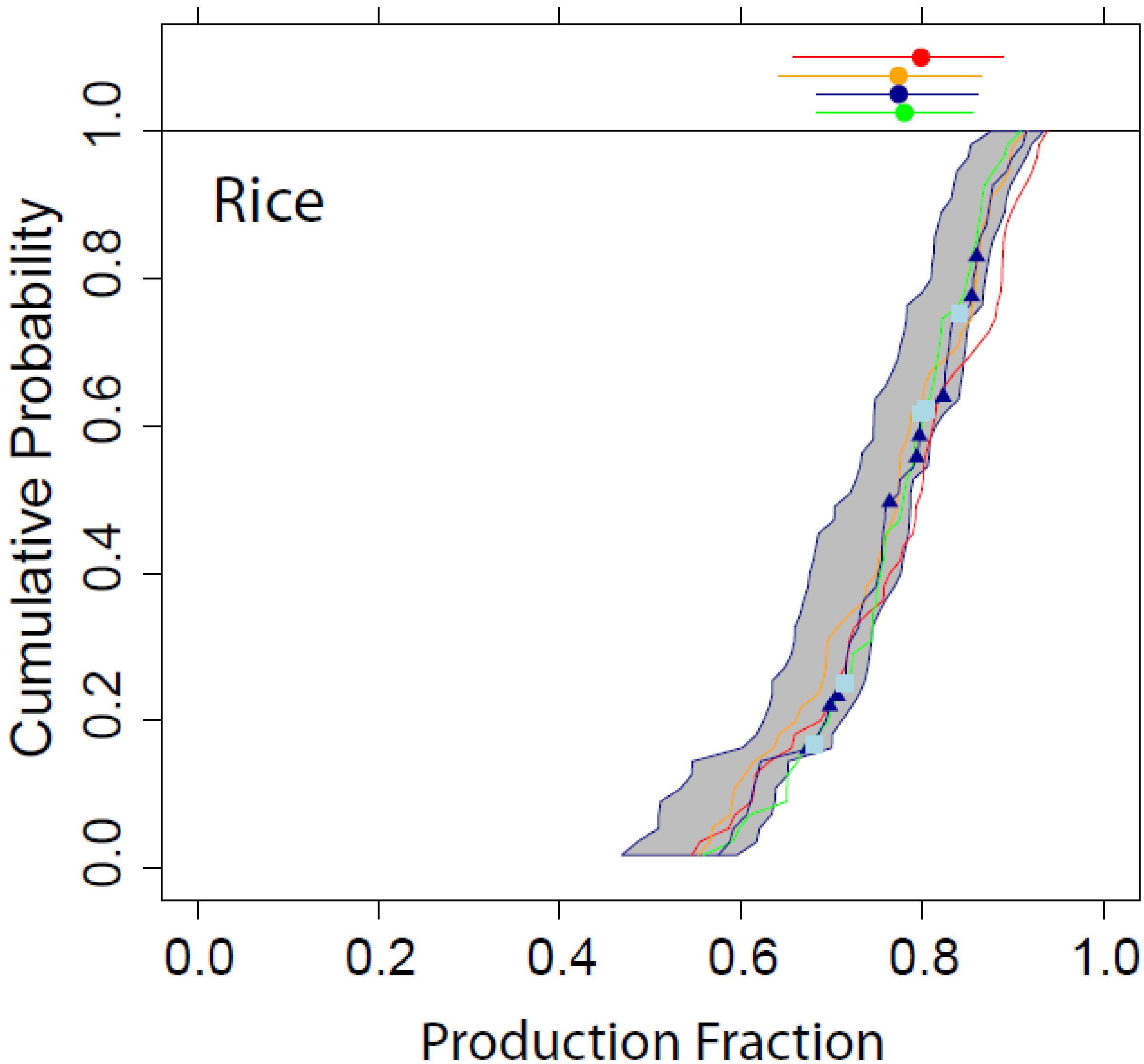
Rice
Cumulative Probability
Production Fraction
0.0
0.2
0.4
0.6
0.8
1.0

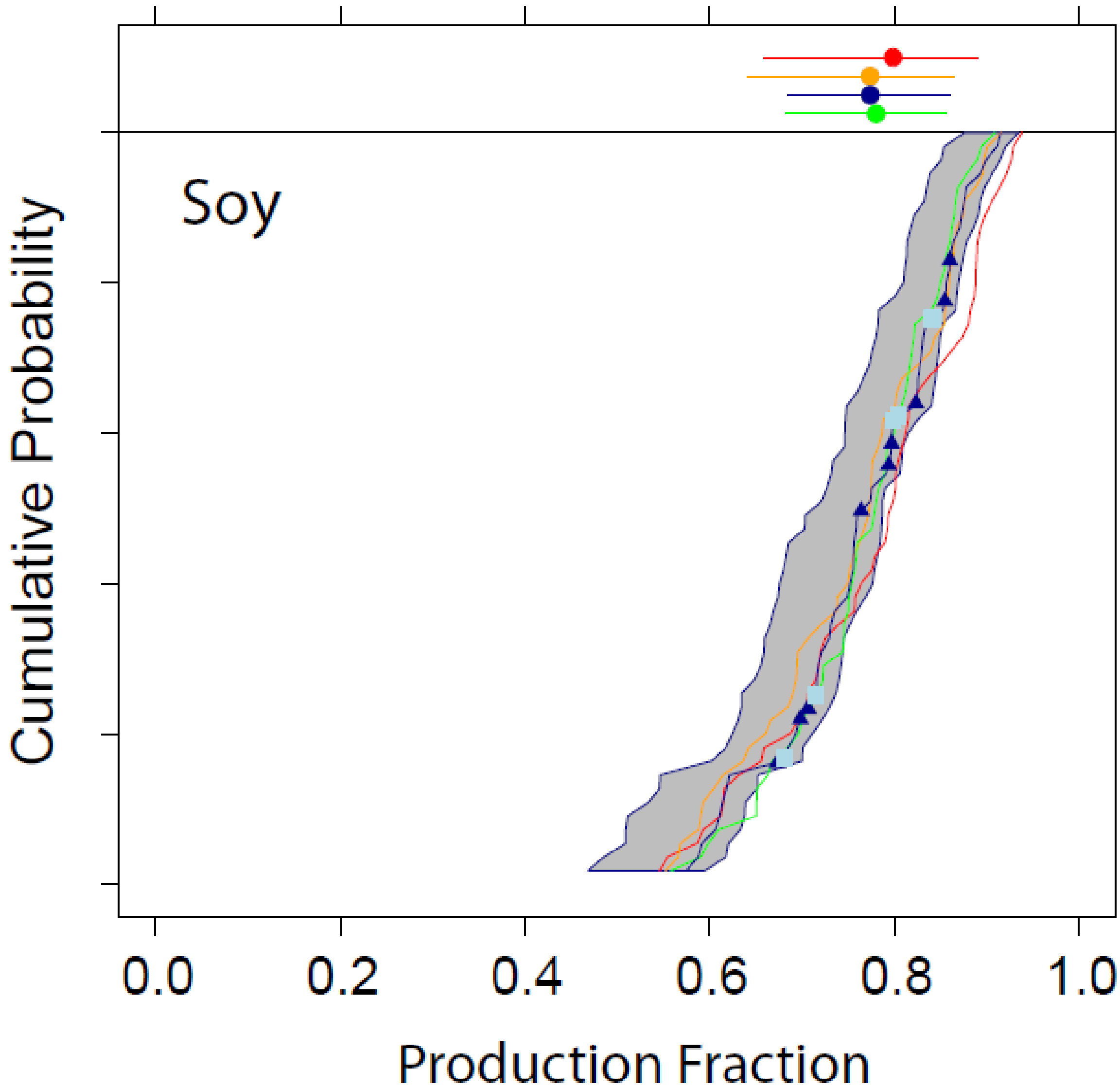

Figure S8. Limits of irrigation according to hydrological models (listed in darkblue) and GGCMs (listed in light blue). The colored lines represent the cumulative probability distribution of the production fraction α at different levels of global warming (green = 1°C, darkblue = 2°C, orange = 3°C, red = 4°C). While the inner lines are based on the ”median” assumption regarding water spent on crops not simulated by LPJmL (Section 3.1 of the SI), the outer lines surrounding the grey shaded area represent results for the ”min” and ”max” setting at 2°C. All results are based on the HadGEM2-ES, RCP8.5 climate input. Lightblue squares: GGCM specific means of α. Darkblue triangles: water model specific means of α. In case of wheat, rice, and soy the GGCM induced spread is comparable to the spread introduced by the hydrological models while for maize the GGCM induced spread is minor. Colored lines at the upper end of the plot represent the inner 66% of the distribution at different levels of global warming. The median is indicated by colored dots.

The production fraction increases non-linearly with the project efficiency. This is due to the optimal distribution of the available water starting from the grid cells where it leads to the highest yield increases per applied amount of water (see Figure S9 below).

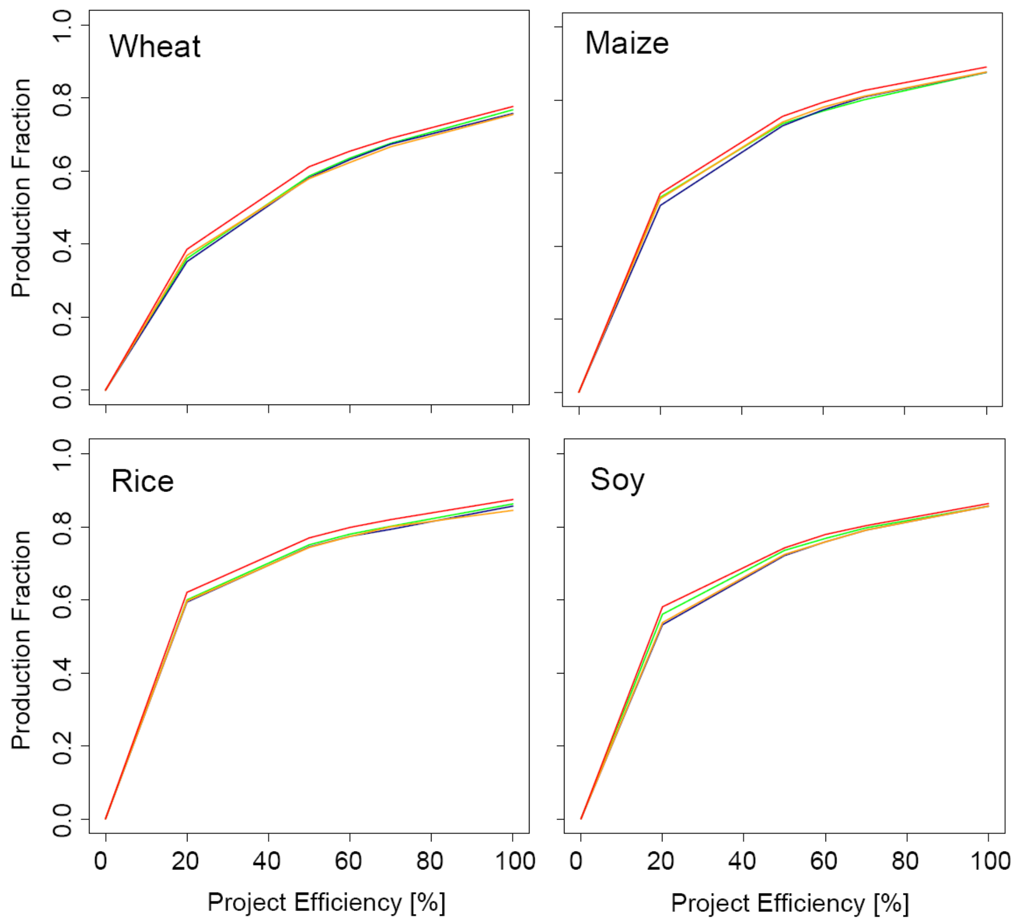

Figure S9. Median production fractions for different project efficiencies (20%, 50%, 60%, 70%, and 100%). Color coding indicates different levels of global warming (green = 1°C, darkblue = 2°C, orange = 3°C, red = 4°C). At a project efficiency of 60% the plotted production fractions corresponds to the median of the cumulative distributions shown above (colored dot in the upper part of each panel).

5. LU changes

5.1 Assumed growth rates within MAgPIE

The annual growth rates due to assumed within MAgPIE to generate the land use patterns used in the paper are time dependent and vary from region to region. The table contains the annual average growth rates for the period 2005-2045 (considered within (Nelson et al., 2013)) and the longer period until 2085 used in this paper. The growth rates are only relevant for the generation of the LU pattern. Crop production changes considered in this paper do not account for these growth rates.

Region	2005-2045	2005-2085
AFR (Sub-Saharan Africa)	4,8%	9,5%
CPA (Central Asia, mainly China)	1,4%	0,7%
EUR (Europe)	0,7%	0,4%
FSU (Former Soviet Union)	0,4%	0,3%
LAM (Latin America)	0,7%	0,9%
MEA (Middle East and North Africa)	3,0%	2,8%
NAM (North America)	1,1%	0,7%
PAO (Pacific OECD countries, Australia, New Zealand, Japan)	1,3%	1,2%
PAS (Pacific Asia)	1,1%	1,0%
SAS (South Asia)	2,2%	2,0%

Table S4. Average annual growth rates of yields used for the generation of the LU patterns by MAgPIE.

5.2 Comparison of MIRCA present day LU patterns to MAgPIE LU future patterns (wheat, maize, rice soy)

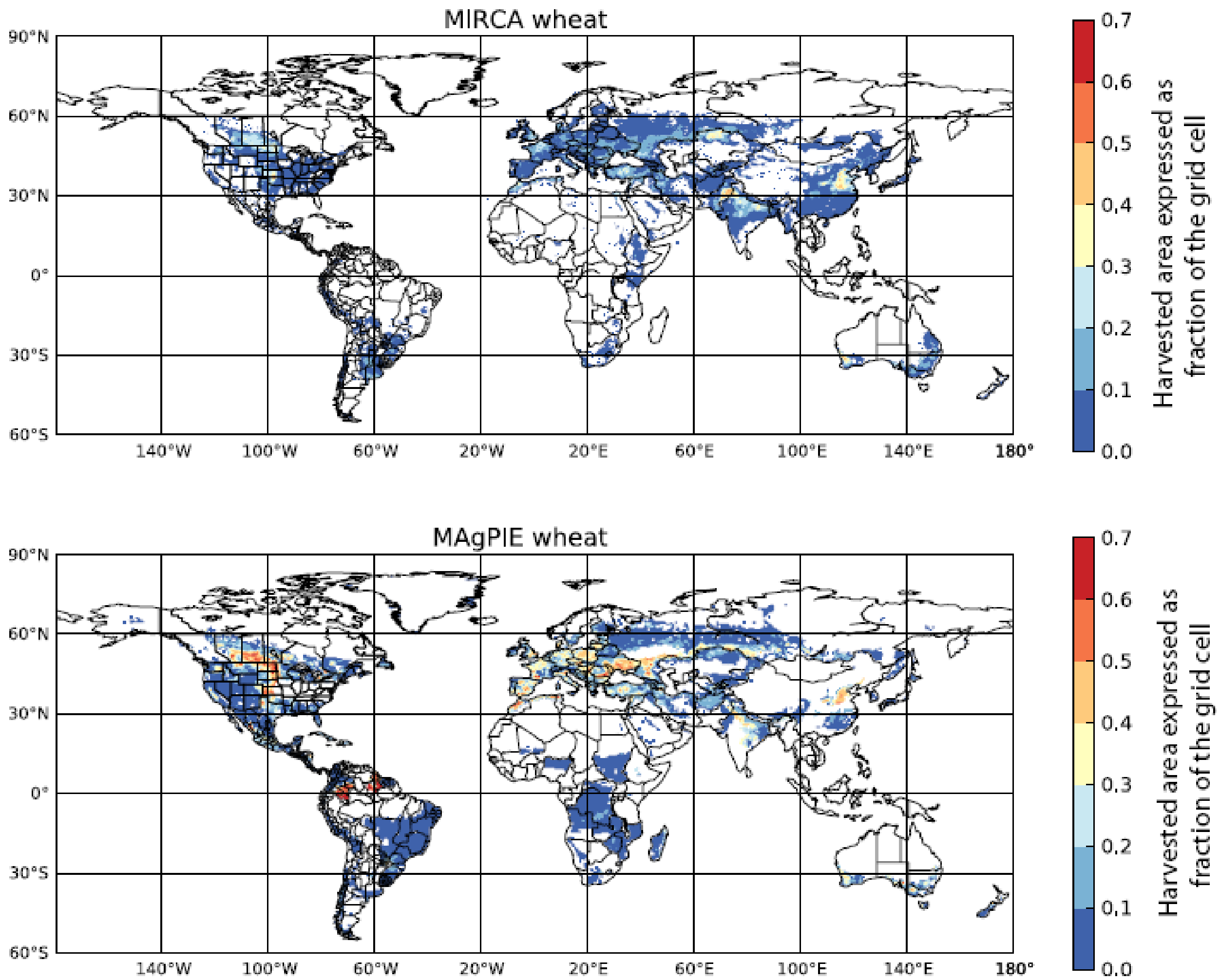

Figure S10: Wheat: Comparison of the “present day” harvested areas as described by the MIRCA data set and the future (2085) physical land area where wheat is grown (which is assumed to be identical to the harvested area in our analysis) as described by the MAgPIE land use model.

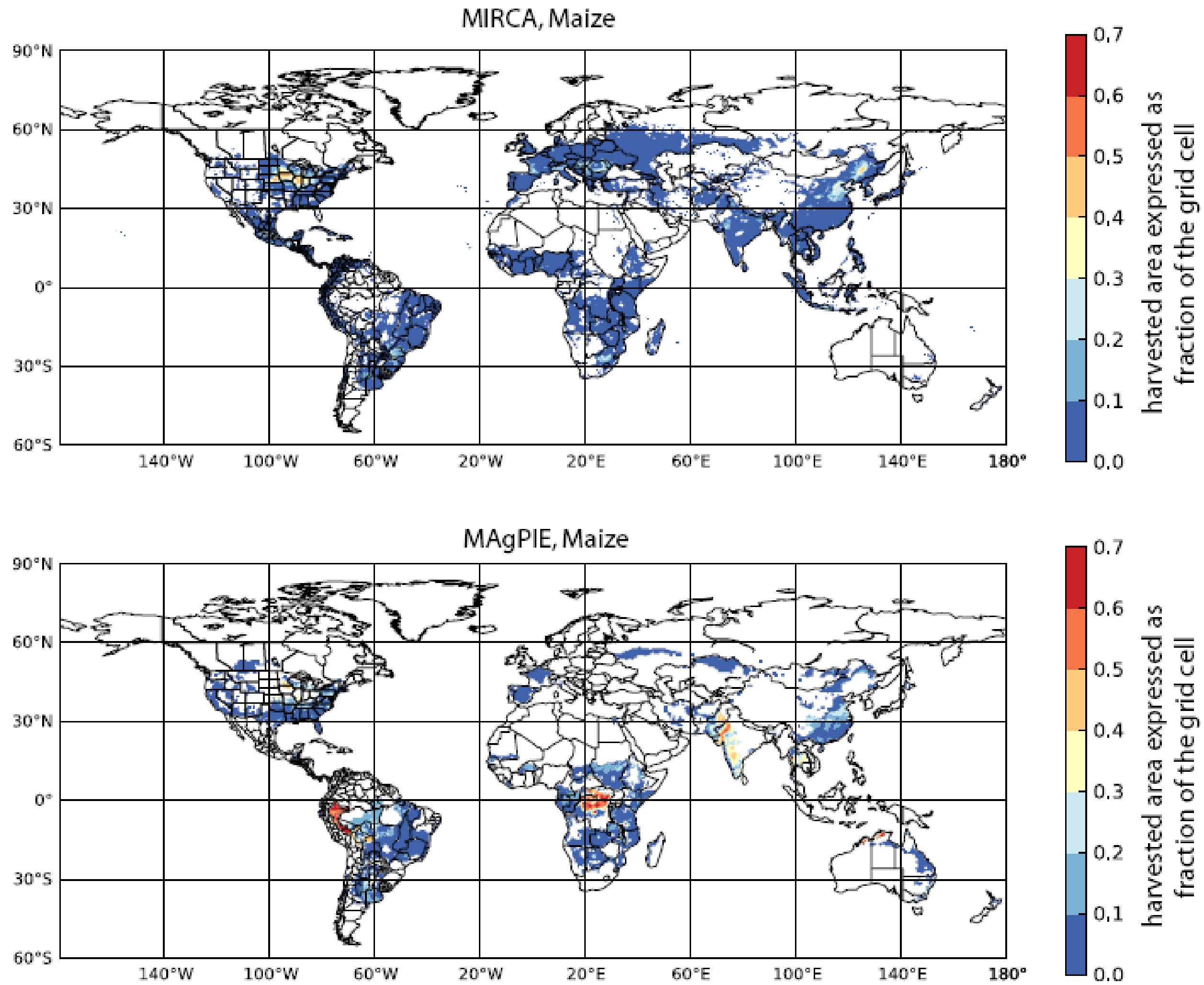

Figure S11: Maize: Comparison of the “present day” harvested areas as described by the MIRCA data set and the future (2085) physical land area where maize is grown (which is assumed to be identical to the harvested area in our analysis) as described by the MAgPIE land use model.

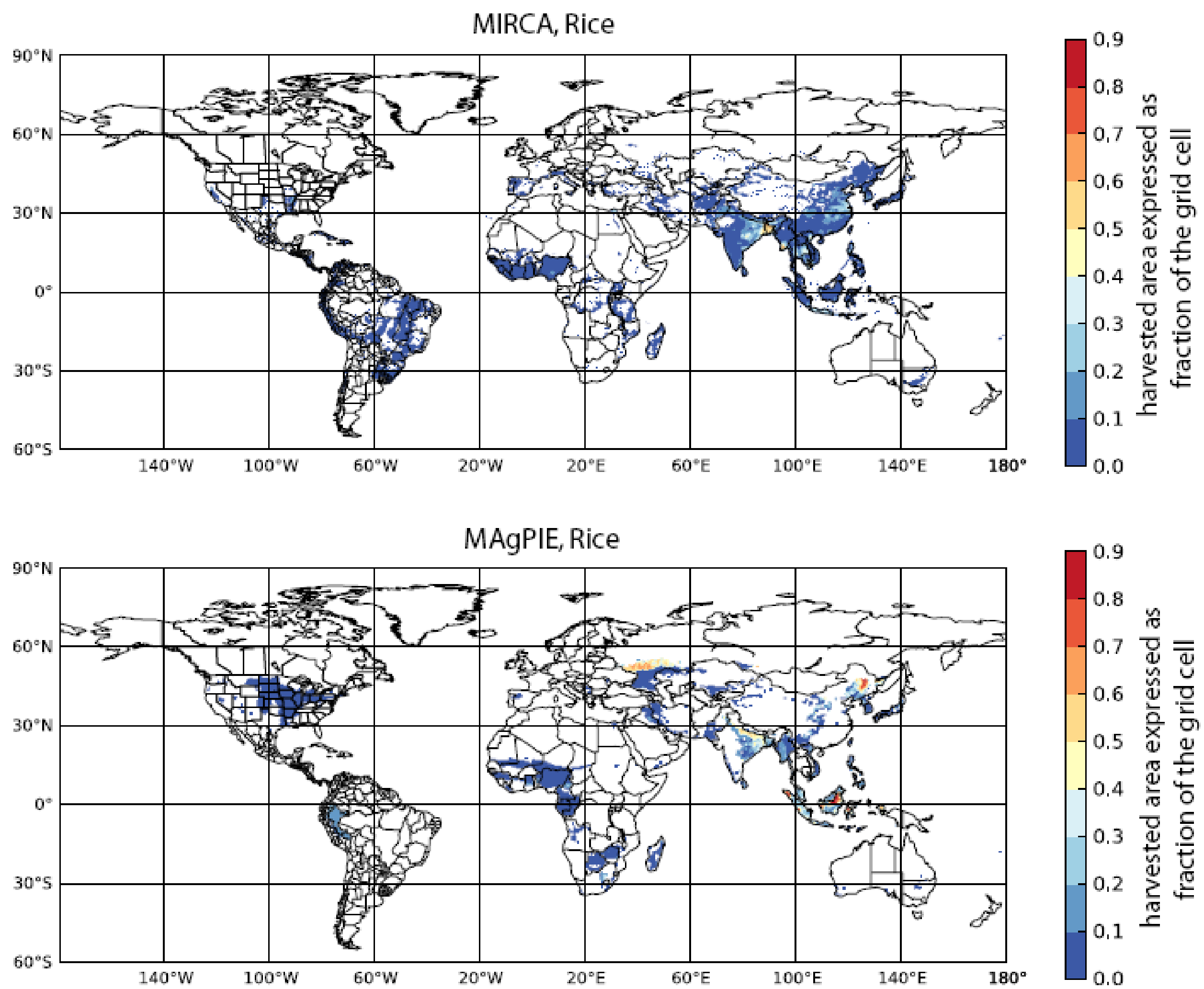

Figure S12: Rice: Comparison of the "present day" harvested areas as described by the MIRCA data set and the future (2085) physical land area where rice is grown (which is assumed to be identical to the harvested area in our analysis) as described by the MAgPIE land use model.

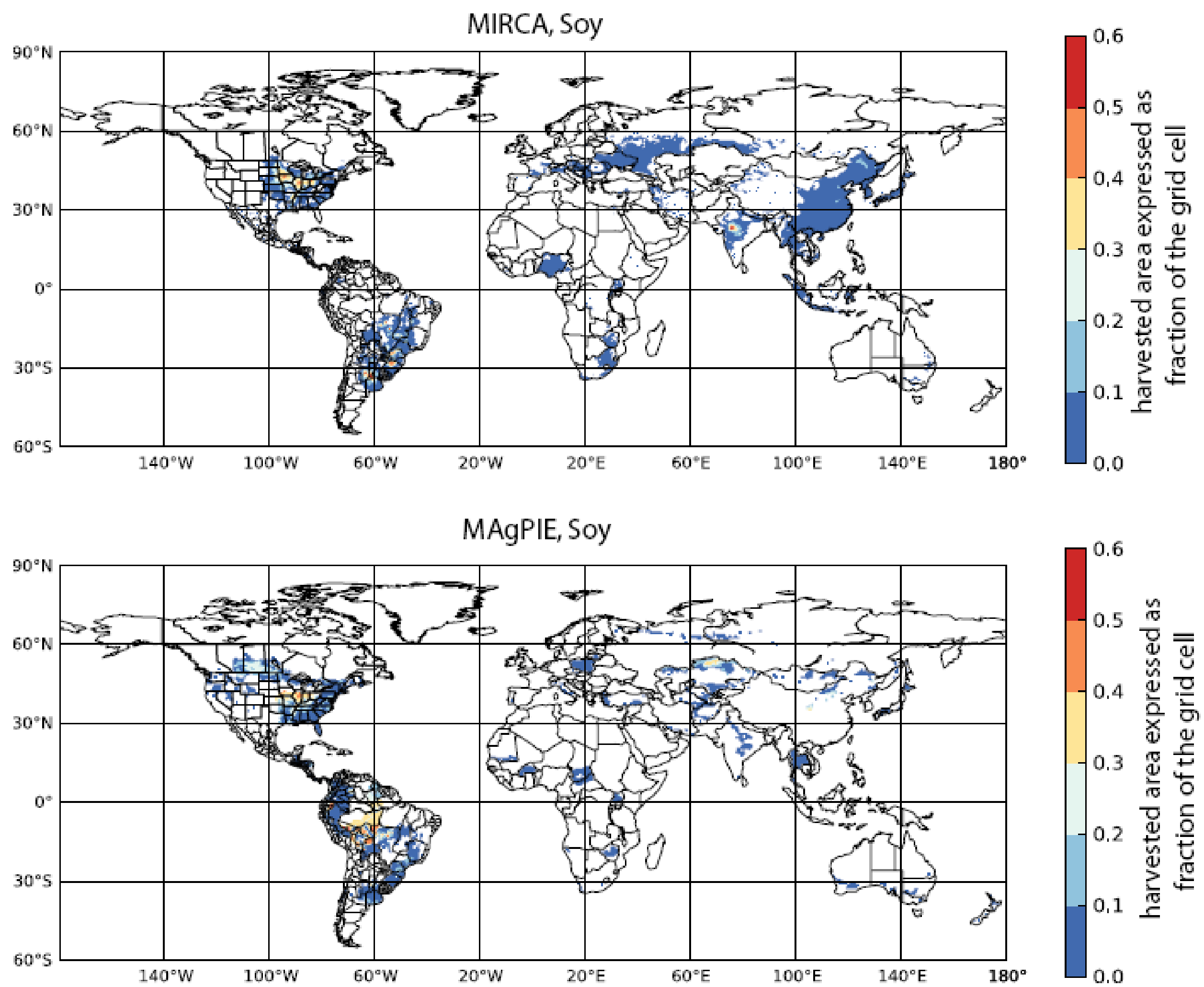

Figure S13: Soy: Comparison of the "present day" harvested areas as described by the MIRCA data set and the future (2085) physical land area where soy is grown (which is assumed to be identical to the harvested area in our analysis) as described by the MAgPIE land use model.

5.3 Loss of natural vegetation

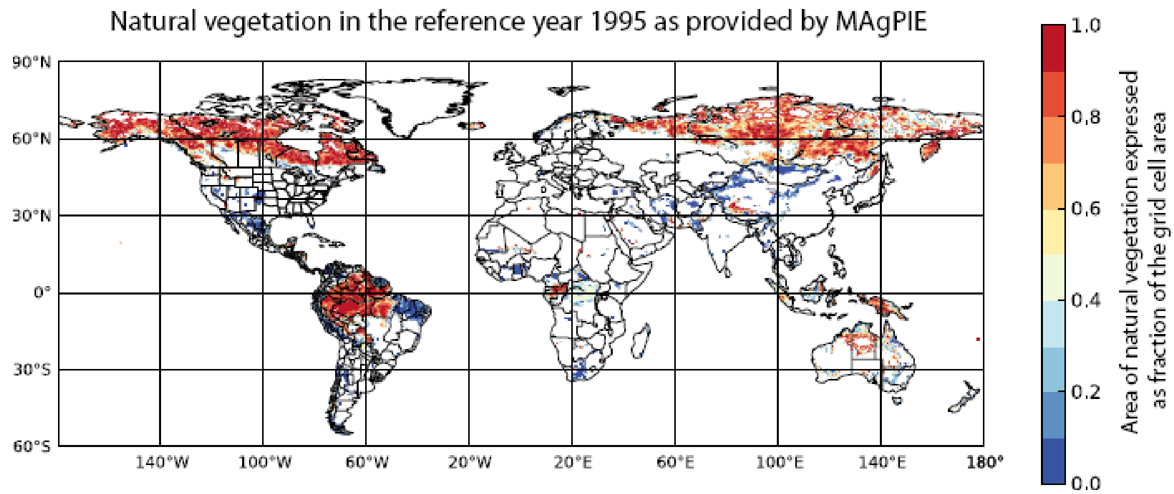

Figure S14: Area of natural vegetation as provided MAgPIE for the reference year 1995.

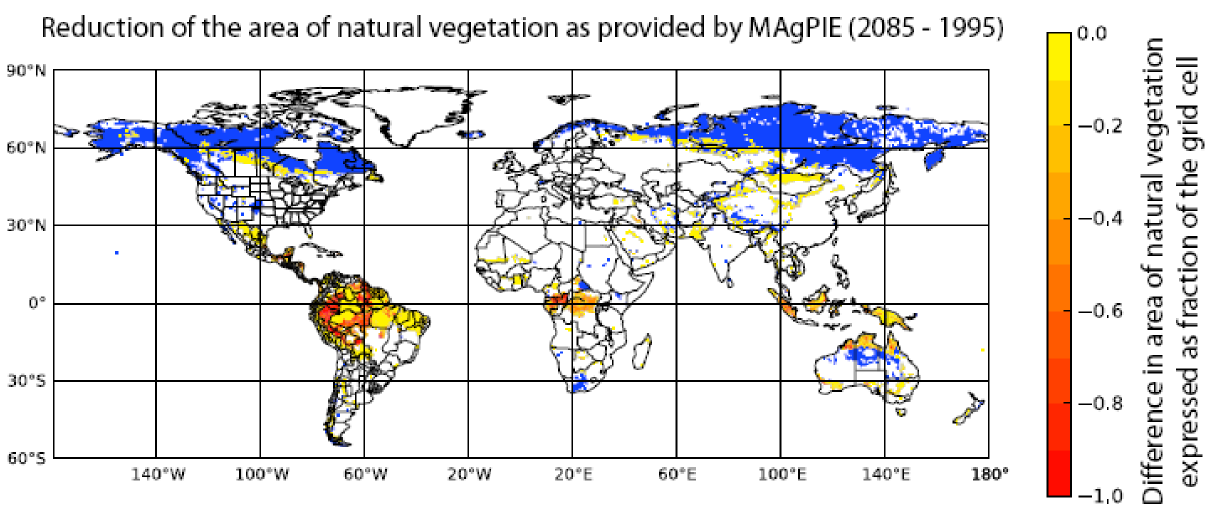

Figure S15: Reduction of the area of natural vegetation as provided by MAGPIE. The map shows the differences between the 2085 fractions of natural vegetation per grid cell and the 1995 fractions (shown in Figure S14 above). Blue areas indicate no changes with respect to the 1995 pattern and yellow to red areas mean reductions with respect to the 1995 reference pattern.

6 Participating bio-geochemical models

Model abbreviation	Representation of dynamic vegetation	Represented bio-geochemical cycles
LPJmL (Gerten et al., 2004; Sitch et al., 2003) Lund-Potsdam-Jena managed Land Dynamic Global Vegetation and Water Balance Model	yes	Representation of a fully coupled water and carbon cycle (assuming optimal leaf nitrogen allocation, but no limitation of CO2 fertilization by nutrient supply)
JULES (Best et al., 2011; Clark et al., 2011) Joint UK Land Environment Simulator	yes	Representation of C cycle (no limitation of CO2 fertilization by nutrient supply e.g. N or P)
JeDI (Pavlick et al., 2013) Jena Diversity Model	yes	representation of water and C cycle, no limitation of CO2 fertilization by nutrient supply
SDGVM (Le Quéré et al., 2009; Woodward et al., 1995) Sheffield Dynamic Vegetation Model	no	fully coupled water and carbon cycle, below ground nitrogen cycle
VISIT (Inatomi et al., 2010; Ito and Inatomi, 2012) Vegetation Integrative Simulation for Trace gases	no	Representation of C and N cycle (but no limitation of CO2 fertilization by N supply in this simulation). For vegetation processes, single vegetation-layer carbon cycle model.
Hybrid (Friend and White, 2000)	yes	Representation of C and N cycles (N provides constraints on photosynthesis, growth, and affects allocation of C to leaf area)
ORCHIDEE (Krinner, 2005; Piao et al., 2007)	Not in the configuration used for ISI-MIP	Representation of C cycle (no limitation of CO2 fertilization by nutrient supply e.g. N or P) Land surface model – calculates energy fluxes and surface

		temperature on a 30 min time step

Table S5: Basic characteristics and references for the bio-geochemical models participating in ISI-MIP and used in this paper to calculate the loss of carbon sinks, reduction of the vegetation carbon stock and the area under risk of severe ecosystem changes.

7 Changes in Ecosystem Atmosphere C Fluxes under the fixed 1995 LU pattern

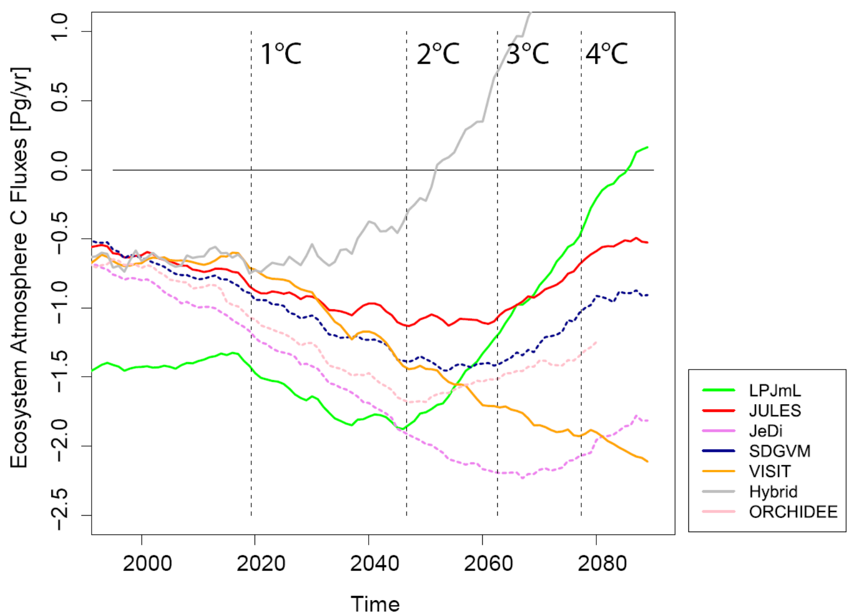

Figure S16: Changes in carbon sinks (ecosystem-atmosphere C flux) integrated over the fixed 1995 area of natural vegetation representing the reference situation of the MAgPIE LU patterns. Dashed lines indicate Biomes models not allowing for dynamical vegetation changes. Simulations are based on HadGEM2-ES, hist+ RCP8.5 climate input. Dashed vertical lines indicate the year where the global mean warming with respect to the reference period 1980-2010 reaches the 1, 2, 3, and 4°C level.

8 Loss of carbon sinks and stocks under constant CO2 conditions

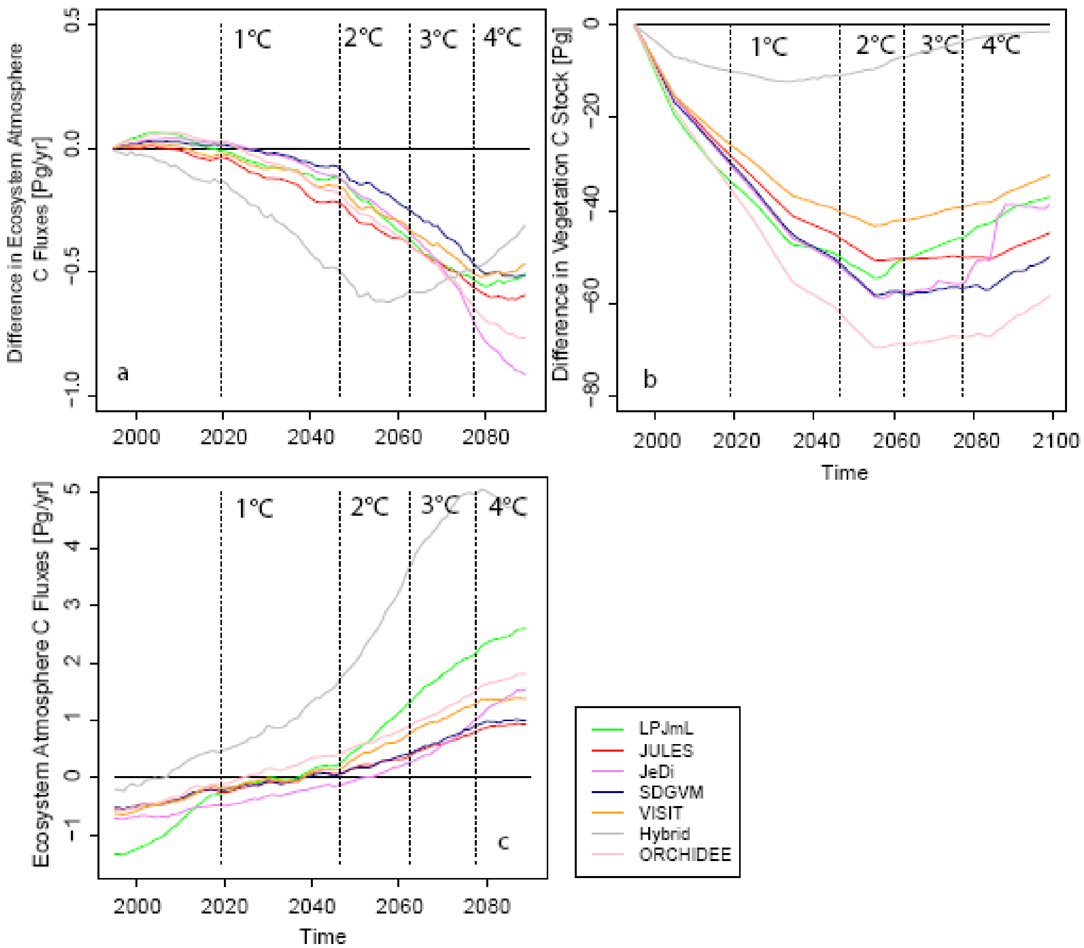

Figure S17: Difference in (a) ecosystem-atmosphere C fluxes (b) the vegetation carbon stock between the scenario where the area of natural vegetation is reduced according to the MAgPIE projections and the reference scenario where the area of natural vegetation is assumed to remain constant (1995 pattern). For reference panel (c) shows the Ecosystem-Atmosphere C fluxes for the fixed 1995 pattern of natural vegetation. All results are based on the simulations under fixed present day CO2 concentrations. The Figure is analogous to Panel a and b of Figure 4 of the main text and based on HadGEM2-ES, hist+ RCP8.5 climate input. Dashed vertical lines indicate the year where the global mean warming with respect to the reference period 1980-2010 reaches the 1, 2, 3, and 4°C level.

9 References for the applied climate models

Institute	Abbreviation	used model version
Met Office Hadley Centre (additional HadGEM2-ES realizations contributed by Instituto Nacional de Pesquisas Espaciais)	MOHC (additional realizations by INPE)	HadGEM2-ES
Institut Pierre-Simon Laplace	IPSL	IPSL-CM5A-LR
Japan Agency for Marine-Earth Science and Technology, Atmosphere and Ocean Research Institute (The University of Tokyo), and National Institute for Environmental Studies	MIROC	MIROC-ESM-CHEM

Table S6: All impact simulations are based on the climate projections based on the above 3 models. Daily data as provided via the CMIP5 archive were bias corrected and provided to all modeling groups participating in ISI-MIP. All simulations are based on the available simulations provided for the historical period and the Representative Concentrations Pathways (RCP2.6, RCP4.5, RCP6.0, and RCP8.5 (Moss et al., 2010)).

References

Anon: FAO, 2007 FertiSTAT - Fertilizer Use Statistics. Food and Agricultural Organization of the UN. Rome., [online] Available from: http://www.fao.org/ag/agl/fertistat/index_en.htm., n.d.

Arnell, N. W.: A simple water balance model for the simulation of streamflow over a large geographic domain, J. Hydrol, 217, 314–335, 1999.

Van Beek, L. P. H., Wada, Y. and Bierkens, M. F. P.: Global monthly water stress: 1. Water balance and water availability, Water Resour. Res., 47(W07517.), 2011.

Best, M. J., Pryor, M., Clark, D. B., Rooney, G. G., Essery, R. . L. H., Ménard, C. B., Edwards, J. M., Hendry, M. a., Porson, a., Gedney, N., Mercado, L. M., Sitch, S., Blyth, E., Boucher, O., Cox, P. M., Grimmond, C. S. B. and Harding, R. J.: The Joint UK Land Environment Simulator (JULES), model description – Part 1: Energy and water fluxes, Geosci. Model Dev., 4(3), 677–699, doi:10.5194/gmd-4-677-2011, 2011.

Bondeau, A., Smith, P. C., Zaehle, S., Schaphoff, S., Lucht, W., Cramer, W., Gerten, D., Lotze-Campen, H., Müller, C., Reichstein, M. and Smith, B.: Modelling the role of agriculture for the 20th century global terrestrial carbon balance, Glob. Chang. Biol., 13(3), 679–706, doi:10.1111/j.1365-2486.2006.01305.x, 2007.

Clark, D. B., Mercado, L. M., Sitch, S., Jones, C. D., Gedney, N., Best, M. J., Pryor, M., Rooney, G. G., Essery, R. L. H., Blyth, E., Boucher, O., Harding, R. J., Huntingford, C. and Cox, P. M.: The Joint UK Land Environment Simulator (JULES), model description – Part 2: Carbon fluxes and vegetation dynamics, Geosci. Model Dev., 4(3), 701–722, doi:10.5194/gmd-4-701-2011, 2011.

Deryng, D., Sacks, W. J., Barford, C. C. and Ramankutty, N.: Simulating the effects of climate and agricultural management practices on global crop yield, Global Biogeochem. Cycles, 25(2), 1–18, doi:10.1029/2009GB003765, 2011.

Döll, P., Hoffmann-Dobrev, H. Portmann, F. T., Siebert, S., Eicker, A., Rodell, M., Strassberg, G. and Scanlon, B.: Impact of water withdrawals from groundwater and surface water on continental water storage variations. doi:10.1016/j.jog.2011.05.001, J. Geodyn., 59-60, 143–156, doi:doi:10.1016/j.jog.2011.05.001, 2012.

Döll, P., Kaspar, F. and Lehner, B.: A global hydrological model for deriving water availability indicators: model tuning and validation., J. Hydrol., 270(1-2), 105–134, 2003.

Fader, M., Rost, S., Müller, C., Bondeau, A. and Gerten, D.: Virtual water content of temperate cereals and maize: Present and potential future patterns, J. Hydrol., 384(3-4), 218–231, doi:10.1016/j.jhydrol.2009.12.011, 2010.

Fereres, E. and Soriano, M. A.: Deficit irrigation for reducing agricultural water use., J. Exp. Bot., 58(2), 147–59, doi:10.1093/jxb/erl165, 2007.

Flörke, M., Kynast, E., Bärlund, I., Eisner, S., Wimmer, F. and Alcamo, J.: Domestic and industrial water uses of the past 60 years as a mirror of socio-economic development: A global simulation study., Glob. Environ. Chang., doi:doi:10.1016/j.gloenvcha.2012.10.018., 2012.

Friend, A. D. and White, A.: Evaluation and analysis of a dynamic terrestrial ecosystem model under preindustrial conditions at the global scale, Global Biogeochem. Cycles, 14(4), 1173–1190, 2000.

Gerten, D., Heinke, J., Hoff, H., Biemanns, H., Fader, M. and Waha, K.: Global water availability and requirements for future food production, J. Hydrometeorol., 12, 885–899, 2011.

Gerten, D., Schaphoff, S., Haberlandt, U., Lucht, W. and Sitch, S.: Terrestrial vegetation and water balance—hydrological evaluation of a dynamic global vegetation model, J. Hydrol., 286(1-4), 249–270, doi:10.1016/j.jhydrol.2003.09.029, 2004.

Gosling, S. N. and Arnell, N. W.: Simulating current global river runoff with a global hydrological model: model revisions, validation and sensitivity analysis., Hydrol. Process., 25, 1129–1145, doi:doi: 10.1002/hyp.7727, 2011.

Hagemann, S. and Gates, L. D.: Improving a subgrid runoff parameterization scheme for climate models by the use of high resolution data derived from satellite observations, Clim. Dyn., 21, 349–359, 2003.

Hanasaki, N., Kanae, S., Oki, T., Masuda, K., Motoya, K., Shirakawa, N., Shen, Y. and Tanaka, K.: An integrated model for the assessment of global water resources – Part 2: Applications and assessments, Hydrol. Earth Syst. Sci., 12(4), 1027–1037, doi:10.5194/hess-12-1027-2008, 2008.

Hanasaki, N., Kanae, S., Oki, T., Masuda, K., Motoya, K., Shirakawa, N. and Shen, Y., and Tanaka, K.: An integrated model for the assessment of global water resources - Part 1: Model description and input meteorological forcing, Hydrol. Earth Syst. Sci., 12, 1007–1025, 2008.

Inatomi, M., Ito, A., Ishijima, K. and Murayama, S.: Greenhouse Gas Budget of a Cool-Temperate Deciduous Broad-Leaved Forest in Japan Estimated Using a Process-Based Model, Ecosystems, 13(3), 472–483, doi:10.1007/s10021-010-9332-7, 2010.

Ito, a. and Inatomi, M.: Use of a process-based model for assessing the methane budgets of global terrestrial ecosystems and evaluation of uncertainty, Biogeosciences, 9(2), 759–773, doi:10.5194/bg-9-759-2012, 2012.

Izaurralde, R. C., Williams, J. R., McGill, W. B., Rosenberg, N. J. and Jakas, M. C. Q.: Simulating soil C dynamics with EPIC: Model description and testing against long-term data, Ecol. Modell., 192(3-4), 362–384, 2006.

Krinner, G.: A dynamic global vegetation model for studies of the coupled atmosphere-biosphere system, Global Biogeochem. Cycles, 19(1), GB1015, doi:10.1029/2003GB002199, 2005.

Kummu, M., Ward, P., de Moel, H. and Varis, O.: Is physical water scarcity a new phenomenon? global assessment of water shortage over the last two millennia, Environ. Res. Lett., 5, 2010.

Leemans, R. and Solomon, A. M.: Modeling the potential change in yield and distribution of the earth's crops under a warmed climate, Clim. Res., 3, 79–96, 1993.

Liang, X. and Lettenmaier, D. P.: A simple hydrologically based model of land surface and energy fluxes for general circulation models, J. Geophys. Res., 99(D7), 14,415 – 14, 428, 1994.

Lindeskog, M., Arneth, A., Bondeau, A., Waha, K., Schurgers, G., Olin, S. and Smith, B.: Effects of crop phenology and management on the terrestrial carbon cycle: case study for Africa, Earth Syst. Dynam. Discuss., 4(2), 235–278, 2013.

Liu, J. G., Zehnder, A. J. B. and Yang, H.: Global crop water use and virtual water trade: the importance of green water, Water Resour. Res., 45, doi:doi.10.1029/2007WR006051., 2009.

Lohmann, D., Raschke, E., Nijssen, B. and Lettenmaier, D. P.: Regional scale hydrology: I. Formulation of the VIC-2L model coupled to a routing model, Hydrol. Sci. J., 43(1), 131–141, 1998.

Moss, R. H., Edmonds, J. A., Hibbard, K. A., Manning, M. R., Rose, S. K., van Vuuren, D. P., Carter, T. R., Emori, S., Kainuma, M., Kram, T., Meehl, G. A., Mitchell, J. F. B., Nakicenovic, N., Riahi, K., Smith, S. J., Stouffer, R. J., Thomson, A. M., Weyant, J. P. and Wilbanks, T. J.: The next generation of scenarios for climate change research and assessment, Nature, 463, 747–756, 2010.

Nelson, G. C., Ahammad, H., Deryng, D., Elliott, J., Fujimori, S., Havlik, P., Heyhoe, E., Page, K., von Lampe, M., Lotze-Campen, H., Daniel Mason, D., van Meijl, H., van der Mensbrugghe, D., Müller, C., Robertson, R., Sands, R. D., Schmid, E., Schmitz, C., Tabeau, A., Valin, H., Willenbockel, D., Rosenzweig, C., Ruane, A. C., Arneth, A., Boote, K. J., Folberth, C., Glotter, M., Khabarov, N., Neumann, K., Piontek, F., Pugh, T. A. M., Stehfest, E., Yang, H. and Jones, J. W.: Climate change effects on agriculture: Economic responses to biophysical shocks, PNAS, 111(9), 3268–3273, doi:10.1073/ pnas.1222463110, 2013.

Pavlick, R., Drewry, D. T., Bohn, K., Reu, B. and Kleidon, A.: The Jena Diversity-Dynamic Global Vegetation Model (JeDi-DGVM): a diverse approach to representing terrestrial biogeography and biogeochemistry based on plant functional trade-offs, Biogeosciences, 10, 4137–4177, doi:doi:10.5194/bg-10-4137-2013, 2013.

Piao, S., Friedlingstein, P., Ciais, P., de Noblet-Ducoudré, N., Labat, D. and Zaehle, S.: Changes in climate and land use have a larger direct impact than rising CO2 on global river runoff trends., Proc. Natl. Acad. Sci. U. S. A., 104(39), 15242–7, doi:10.1073/pnas.0707213104, 2007.

Pokhrel, Y., Hanasaki, N., Koirala, S., Cho, J., Yeh, P. J. F., Kim, H., Kanae, S. and Oki, T.: Incorporating anthropogenic water regulation modules into a land surface model, J. Hydrometeorol., 13(1), 255–269, 2012.

Portmann, F. T., Siebert, S. and Döll, P.: MIRCA2000—Global monthly irrigated and rainfed crop areas around the year 2000: A new high-resolution data set for agricultural and hydrological modeling, Global Biogeochem. Cycles, 24(1), GB1011, doi:10.1029/2008GB003435, 2010.

Le Quéré, C., Raupach, M. R., Canadell, J. G., Marland et al., G., Le Quéré et al., C., Marland, G., Bopp, L., Ciais, P., Conway, T. J., Doney, S. C., Feely, R. a., Foster, P., Friedlingstein, P., Gurney, K., Houghton, R. a., House, J. I., Huntingford, C., Levy, P. E., Lomas, M. R., Majkut, J., Metzl, N., Ometto, J. P., Peters, G. P., Prentice, I. C., Randerson, J. T., Running, S. W., Sarmiento, J. L., Schuster, U., Sitch, S., Takahashi, T., Viovy, N., van der Werf, G. R. and Woodward, F. I.: Trends in the sources and sinks of carbon dioxide, Nat. Geosci., 2(12), 831–836, doi:10.1038/ngeo689, 2009.

Rost, S., Gerten, D., Bondeau, A., Lucht, W., Rohwer, J. and Schaphoff, S.: Agricultural green and blue water consumption and its influence on the global water system, Water Resour. Res., 44(9), 1–17, doi:10.1029/2007WR006331, 2008.

Sitch, S., Smith, B., Prentice, I. C., Arneth, a., Bondeau, a., Cramer, W., Kaplan, J. O., Levis, S., Lucht, W., Sykes, M. T., Thonicke, K. and Venevsky, S.: Evaluation of ecosystem dynamics, plant geography and terrestrial carbon cycling in the LPJ dynamic global vegetation model, Glob. Chang. Biol., 9(2), 161–185, doi:10.1046/j.1365-2486.2003.00569.x, 2003.

Stacke, T. and Hagemann, S.: Development and validation of a global dynamical wetlands extent scheme. Hydrol. Earth Syst. Sci., Hydrol. Earth Syst. Sci., 16, 2915–2933, 2012.

Takata, K., Emori, S. and Watanabe, T.: Development of the minimal advanced treatments of surface interaction and runoff, Glob. Planet. Chang., 38(1), 209–222, 2003.

Tang, Q., Oki, T., Kanae, S. and H. Hu: The influence of precipitation variability and partial irrigation within grid cells on a hydrological simulation, J. Hydrometeorol., 8, 499–512, 2007.

Tang, Q., Oki, T., Kanae, S. and Hu, H.: Hydrological cycles change in the Yellow River Basin during the last half of the 20th century, J. Clim., 21(8), 1790–1806., 2008.

Vörösmarty, C. J., Peterson, B. J. and Lammers, R. B., Shiklomanov, I. A.: A regional, electronic Hydrometeorlogical Water Balance Model data network for the pan-Arctic Region, [online] Available from: Retrieved from http://www.r-arcticnet.sr.unh.edu, 1998.

Wada, Y., Beek, L. P. H. van, Kempen, C. M. van, Reckman, J. W. T. M., Vasak, S. and Bierkens, M. F. P.: Global depletion of groundwater resources., Geophys. Res. Lett., L20402., 2010.

Waha, K., van Bussel, L., Müller, C. and Bondeau, A.: Climate-driven simulation of global crop sowing dates, Glob. Ecol. Biogeogr., 21, 247–259, 2012.

Williams, J. R.: The EPIC Model. In: V.P. Singh (eds). Computer Models of Watershed Hydrology., Water Resour. Publ. Highl. Ranch, Color., 909–1000, 1995.

Williams, J. R., Jones, C. A., Kiniry, J. R. and Spanel, D. A.: The EPIC crop growth model, Trans ASAE, 32, 497–511, 1989.

Wisser, D., Fekete, B. M., Vörösmarty, C. J. and Schumann, A. H.: Reconstructing 20th century global hydrography: A contribution to the Global Terrestrial Network-Hydrology (GTN-H). Hydrology and Earth System Sciences doi:10.5194/hess-14-1-010, Hydrol. Earth Syst. Sci., 14(1), 1–24, doi:doi:10.5194/hess-14-1-010, 2010.

Woodward, F. I., Smith, T. M. and Emanuel, W. R.: A global land primary productivity and phytogeography model, Global Biogeochem. Cycles, 9(4), 471–490, 1995.